



ESCUELA TÉCNICA SUPERIOR DE INGENIERÍA  
(ICAI)

Máster de Ingeniería Industrial y Máster de Industria  
inteligente

**Pattern Recognition in Myoelectric Signals**  
*Embedded Sensorization and Deep Learning Based  
Classification for Prosthetic Control*

Author:

A. Quintana Criado

Direction:

Dr. Romano Giannetti

Dr. Jose Daniel Muñoz Frias

Madrid

Jul 2024



**Alberto Quintana Criado**, declara bajo su responsabilidad, que el Proyecto con título **Pattern Recognition in Myoelectric Signals** presentado en la ETS de Ingeniería (ICAI) de la Universidad Pontificia Comillas en el curso académico 2020/21 es de su autoría, original e inédito y no ha sido presentado con anterioridad a otros efectos. El Proyecto no es plagio de otro, ni total ni parcialmente y la información que ha sido tomada de otros documentos está debidamente referenciada.

Fdo.: .....  ..... Fecha: 16 / Julio / 2024

Autoriza la entrega:

EL DIRECTOR DEL PROYECTO

Nombre del Co - Director 1

Fdo.: .....  ..... Fecha: 16 / 7 / 2024

Nombre del Co - Director 2

Fdo.: .....  ..... Fecha: 16 / 7 / 2024

V. B. DEL COORDINADOR DE PROYECTOS

Nombre del Coordinador

Fdo.: ..... Fecha: ..... / ..... / .....





ESCUELA TÉCNICA SUPERIOR DE INGENIERÍA  
(ICAI)

Máster de Ingeniería Industrial y Máster de Industria  
inteligente

**Pattern Recognition in Myoelectric Signals**  
*Embedded Sensorization and Deep Learning Based  
Classification for Prosthetic Control*

Author:

A. Quintana Criado

Direction:

Dr. Romano Giannetti

Dr. Jose Daniel Muñoz Frias

Madrid

Jul 2024



# Resumen

## Introducción

El siguiente resumen dará una breve explicación del trabajo realizado por Alberto Quintana Criado durante su tesis de Máster, en el cual el proyecto se entrelazó con un proyecto general en el contexto de una colaboración entre el Hospital Universitario de Getafe y el Departamento de Electrónica y Automática de ICAI.

En este proyecto se concibió, diseñó, fabricó y probó con éxito un prototipo 3 de un dispositivo grabador de sEMG, así como versiones más avanzadas del mismo. El mismo conjunto de prototipos se utilizó como grabador de sEMG e implantado respectivamente en los sujetos animales con éxito. Después de eso, se probó un modelo de DL donde el conjunto de datos era un conjunto de datos de sEMG disponible públicamente de amputados transhumerales, demostrando aún más y comparando modelos ligeros para ver cuál podría usarse más adelante en el desarrollo.

## Objetivos:

Los principales objetivos de este proyecto son los siguientes:

1. Desarrollo de un dispositivo de grabación de sEMG según las especificaciones necesarias para el proyecto y los actores principales, así como emplear las habilidades de diseño electrónico e IoT aprendidas durante el MEng.
2. Desarrollo de un banco de pruebas de DL de modelos simples para la comparación y también para determinar la usabilidad en futuros casos, así como en este proyecto más adelante.
3. Idear aplicaciones futuras potenciales o caminos de investigación para esta tecnología, así como servir como base para futuros desarrollos.

Con estos simples objetivos, el proyecto completo se dividió en 3 capítulos correspondientes, cada uno enfocado en la ejecución del objetivo en cuestión.



Figure 1: Aspecto final de la parte de grabación analógica del dispositivo de grabación sEMG diseñado en este proyecto.

## Solución:

### Capítulo 1: Contexto del Proyecto, Diseño y pruebas de una Interfaz Hombre-Máquina

La naturaleza del sEMG y otras bioseñales proviene del uso del cuerpo humano de medios eléctricos y químicos de comunicación. Estas señales se llaman Potenciales de Acción y, en esencia, son una descarga causada por la polarización-despolarización de las membranas. Las soluciones ideadas al diseñar el dispositivo de grabación de sEMG fueron las siguientes:

1. **Maximizar la relación señal-ruido:** La señal EMG es muy pequeña (0-10 mV pico a pico o 0-1.5 mV RMS) en comparación con las fuentes de ruido potenciales. Las principales fuentes de ruido incluyen ruido inherente de componentes electrónicos, ruido electromagnético ambiental (por ejemplo, 50/60 Hz de las líneas eléctricas), artefactos de movimiento de los electrodos y cables, e interferencia de otros biopotenciales como el ECG. Solucionamos esto utilizando componentes electrónicos de alta calidad y una fase de amplificación, seguida de una fase de filtrado.
2. **Evitar la distorsión de la señal EMG:** La contribución relativa de diferentes componentes de frecuencia en la señal EMG no debe ser alterada por el proceso de grabación. La señal EMG tiene energía utilizable de 0-500 Hz, con energía dominante entre 50-150 Hz. Los filtros utilizados para reducir el ruido deben ser diseñados cuidadosamente. La distorsión debido al retraso es inevitable. Además, este retraso depende de la naturaleza de la amplificación



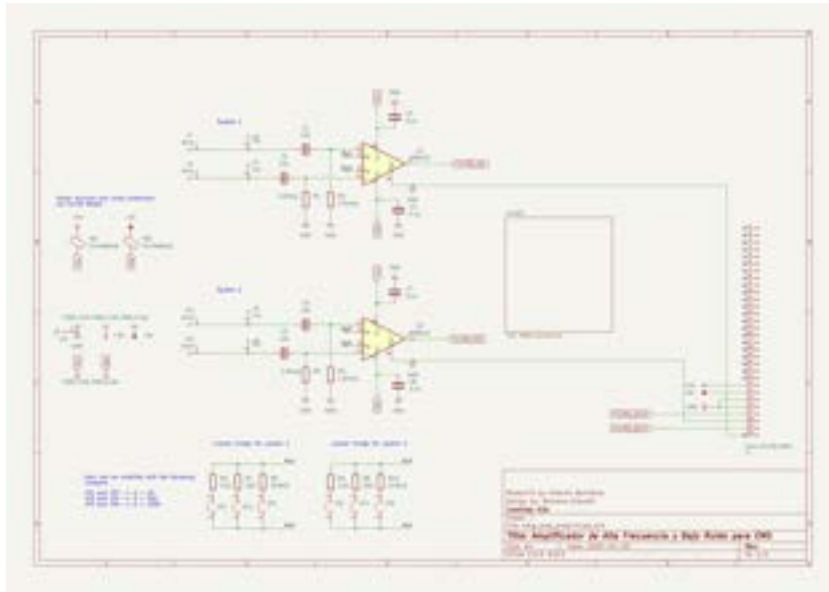


Figure 2: Plano de la fase de amplificación. Muestra una fase de amplificación analógica de sEMG de dos canales. Se tomó la decisión de diseño de incluir dos canales de grabación para aprovechar al máximo la capacidad de doble canal del ADALM-2000.

no lineal en la frecuencia, lo que significa que aparecerá una "distorsión de forma de onda" con diferentes niveles de fase aplicados a diferentes armónicos. Para evitar esto, afinamos las frecuencias en la fase de filtrado para eliminar las bandas innecesarias.

3. **Seleccionar los electrodos apropiados** para la aplicación: Los electrodos superficiales son no invasivos pero tienen limitaciones: solo pueden registrar músculos superficiales, se ven afectados por el tejido subcutáneo y tienen riesgo de interferencia de músculos adyacentes. Los electrodos intramusculares de hilo fino o aguja pueden registrar de músculos profundos y unidades motoras específicas, pero son invasivos. El material, tamaño, forma y distancia entre electrodos afectan la selectividad y calidad de la señal. La elección de electrodos superficiales o intramusculares depende de la aplicación clínica o de investigación específica. [6]

| Modelo              | Pérdida | Precisión | F1    | Precisión |
|---------------------|---------|-----------|-------|-----------|
| Puño                | 2.28    | 0.937     | 0.937 | 0.937     |
| Mano Abierta        | 1.20    | 0.966     | 0.966 | 0.966     |
| Flexión de Muñeca   | 1.10    | 0.969     | 0.969 | 0.969     |
| Extensión de Muñeca | 1.12    | 0.968     | 0.968 | 0.968     |
| Desviación Radial   | 1.13    | 0.968     | 0.968 | 0.968     |
| Desviación Cubital  | 1.17    | 0.967     | 0.967 | 0.967     |

Table 1: Resultados de la prueba del experimento C en la clasificación de 6 etiquetas

## Capítulo 2: Clasificación del comportamiento del EMG en amputados transhumerales a través de aplicaciones de DL

La aplicación particular para este proyecto garantizará la capacidad de los amputados y personas que sufren lesiones traumáticas de no estar limitados en movimiento mediante la aplicación de los descubrimientos del capítulo 1 anterior. Sin embargo, como se explicó, los neuromas representan un problema significativo cuando se realizan análisis debido a la naturaleza especial y a menudo traumática de su aparición. La señal en sí experimentará cambios en su forma, lo que significa propiedades cambiantes tanto en el dominio del tiempo como en el dominio de la frecuencia.

Se eligió y entrenó un conjunto de modelos ligeros de DL capaces de clasificar con precisión y aún tener un tamaño lo suficientemente pequeño como para ejecutarse en la mayoría de los dispositivos tipo IoT.

- Las redes neuronales **LSTM**, **GRU** y **LSTM bidireccional** fueron capaces de inferir parte de la abstracción relacionada con la activación de los diferentes movimientos de la mano con éxito, por otro lado, esta arquitectura de red neuronal no mostró suficiente consistencia en los experimentos. La secuencialidad en la arquitectura demuestra ser ventajosa al procesar los datos, ya que puede ser una ventaja en una aplicación en tiempo real.
- Los modelos basados en **CNN** son más fuertes cuando se trata de manejar la abstracción en señales de sEMG de bajo a medio ruido, demostrando ser ventajosos como el clasificador de elección para este proyecto. Muchos dispositivos IoT hoy en día tienen redes neuronales basadas en visión por computadora capaces de mucho más, lo que habla del potencial de esta tecnología.

## Conclusión y bibliografía:

1. **Utilización y Preprocesamiento de Datos:** La investigación enfatiza la importancia de la naturaleza secuencial de las señales de sEMG, empleando una técnica de ventana deslizante para segmentar los datos de manera efectiva.

2. **Arquitectura y Entrenamiento del Modelo:** El modelo basado en CNN fue seleccionado por su robustez en el manejo de dependencias espaciales y temporales inherentes a los datos de sEMG. La extracción y aumento de características jugaron un papel significativo en la mejora del rendimiento de la clasificación, ya que estos pasos permitieron que el modelo se centrara en patrones críticos dentro de los datos.

3. **Rendimiento y Evaluación:** Aunque el modelo logró una precisión encomiable, permanecieron ciertos desafíos, particularmente en la distinción de movimientos con patrones de activación muscular similares.

4. **Desafíos y Direcciones Futuras:** La transición a un enfoque basado en características destacó varios desafíos, en particular la necesidad de una mayor optimización para mejorar la robustez del modelo contra el ruido y la variabilidad en las señales.

5. **Enfoques Innovadores:** La introducción de un conjunto adicional de variables para mejorar la robustez del modelo contra el ruido es un enfoque novedoso que merece una mayor exploración.

## Implicaciones Prácticas

Los hallazgos de esta investigación tienen implicaciones significativas para el desarrollo de tecnologías asistenciales, particularmente en el campo de las prótesis y la rehabilitación. La clasificación precisa de los movimientos de la mano y la muñeca utilizando señales de sEMG puede llevar a sistemas de control más intuitivos y receptivos para las extremidades protésicas. Los avances en la extracción de características y el entrenamiento de modelos presentados en esta tesis contribuyen al creciente cuerpo de conocimientos destinado a mejorar la calidad de vida de las personas que dependen de dispositivos asistenciales.

Además, a medida que se amplía el alcance de una futura colaboración entre UHG y Comillas ICAI, este POC ha demostrado ser fructífero para determinar el enfoque inicial de esta tecnología y las pruebas a realizar.

## Trabajo Futuro

Aunque este proyecto fue definitivamente un POC para un alcance mayor, aún logra iluminar algunas áreas que pueden tener un impacto profundo en la in-

vestigación. Por lo tanto, los próximos pasos de este POC pueden determinarse fácilmente.

1. **Consumo de energía y disipación de calor:** Optimizar la eficiencia energética y la gestión térmica es fundamental para los dispositivos implantables que requieren largas horas de uso y altas cargas computacionales.
2. **Telemetría y comunicaciones inalámbricas:** Permitir la transmisión inalámbrica de datos es esencial para una telemetría sin problemas y la gestión remota de dispositivos sin procedimientos invasivos.
3. **Preprocesamiento digital:** Integrar el preprocesamiento digital en el microprocesador del implante puede reducir la sobrecarga de transmisión de datos y permitir un análisis de señales en tiempo real más eficiente.

# Abstract

## Introduction

The following abstract will give brief explanation to the work executed by Alberto Quintana Criado during his final Master´s thesis, in which the project was intertwined with an overarching project in the context of a collaboration between UHG (University Hospital of Getafe and the Electronics and Automation Department at ICAI.

In this project a successful prototype 3 for an sEMG recorder device was conceived, designed, manufactured and tested as well as more advanced versions of the same. The same set of prototypes were used as an sEMG recorder and implanted respectively on the animal subjects with success. After that a DL model was tried and tested where the dataset was a publicly available dataset of sEMG signals from trans-humeral amputees, further proving and comparing lightweight models can to see which one could be used further down the line in development.

## Goals:

The main goals of this project are the following:

1. Development of a sEMG recording device according to the specifications needed by the project and the main actors as well as employing the electronics and IoT design skills learned during the MEng.
2. Development of a DL testbench of simple models for comparison and also to determine usability in future cases as well as in this project further down the line.
3. Devise potential future applications or research paths for this technology as well as serving as a stepping ground for future development.

With this simple goals the whole project was divided into 3 corresponding chapter, each one focusing on the execution of the goal in question.

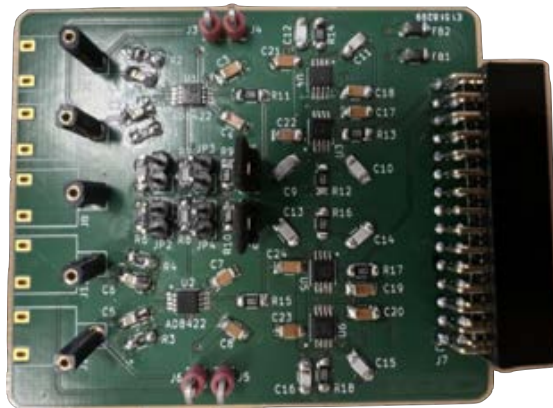


Figure 3: Final look of the Analog Recording part of the prototype sEMG recording device designed in this project.

## Solution:

### Chapter 1: Context of the Project, Design and testing of a Human-Machine Interface

The nature of sEMG and other bio-signals stem from the use of the human body of electric and chemical means of communication. These signals are called Action Potentials and are, at the very core, a discharged caused by the polarization-depolarization of membranes. solutions devised when designning the sEMG recording device where the following:

1. **Maximizing the signal-to-noise ratio:** The EMG signal is very small (0-10 mV peak-to-peak or 0-1.5 mV RMS) compared to potential noise sources. Key noise sources include inherent noise from electronic components, ambient electromagnetic noise (e.g. 50/60 Hz from power lines), motion artifacts from electrodes and cables, and interference from other bio-potentials like ECG. We solved this by using high quality electronics and a amplification phase, followed by a filtering phase.
2. **Avoiding distortion of the EMG signal:** The relative contribution of different frequency components in the EMG signal should not be altered by the recording process. The EMG signal has usable energy from 0-500 Hz, with dominant energy between 50-150 Hz. Filters used to reduce noise must be designed carefully. Distortion due to delay is unavoidable. Furthermore, this delay is dependant due to the nature of non-linear amplification on the frequency, meaning a "waveform distortion" will appear with different levels

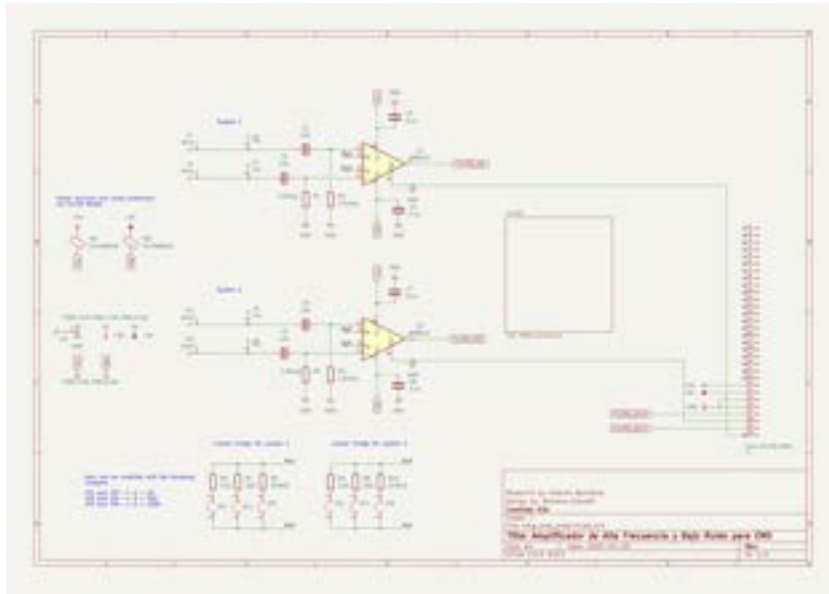


Figure 4: Amplification phase blueprint. It shows a two channel sEMG analog amplifying phase. A choice was made during the design to include two recording channels to make full use of the ADALM-2000 double channel capacity.

of phase being applied on different harmonics. To avoid this we finetuned the frequencies in the filtering phase to remove the unneeded bands.

3. **Selecting appropriate electrodes** for the application: Surface electrodes are non-invasive but have limitations - they can only record superficial muscles, are affected by subcutaneous tissue, and risk cross-talk from adjacent muscles. Intramuscular fine-wire or needle electrodes can record from deep muscles and specific motor units but are invasive. Electrode material, size, shape and inter-electrode distance affect selectivity and signal quality. The choice of surface or intramuscular electrodes depends on the specific clinical or research application. [6]

## Chapter 2: Classifying the behaviour of EMG in trans-humeral amputees through DL applications

The particular application for this project will guarantee the ability for amputees and people suffering from traumatic injuries to not be limited in movement via the application of the discoveries from the previous chapter 1. Nevertheless, as explained, Neuroma pose a significant issue when analysis are performed due to the special and often traumatic nature of their appearance. The signal itself will

| Model            | Loss | Acc   | F1    | Prec  |
|------------------|------|-------|-------|-------|
| Fist             | 2.28 | 0.937 | 0.937 | 0.937 |
| Open Hand        | 1.20 | 0.966 | 0.966 | 0.966 |
| Wrist Flexion    | 1.10 | 0.969 | 0.969 | 0.969 |
| Wrist Extension  | 1.12 | 0.968 | 0.968 | 0.968 |
| Radial Deviation | 1.13 | 0.968 | 0.968 | 0.968 |
| Ulnar Deviation  | 1.17 | 0.967 | 0.967 | 0.967 |

Table 2: Test results of experiment C on 6 label classification

experience changes in its shape meaning shifting properties both in the time-domain and frequency-domain

A set of lightweight DL models capable of classifying accurately and still having a small enough footprint to run in most IoT-like devices was chosen and trained.

- **LSTM, GRU and Bidirectional LSTM** neural networks were capable of inferring some of the abstraction relating to the activation of the different hand movements successfully, on the other hand this neural net architecture did not show enough consistency across experiments. Sequentiality in the architecture proves advantageous when processing the data, as it may be an advantage in a real time application.
- **CNN-based** models are stronger when it comes to handling abstraction in low to medium noise sEMG signals, proving advantageous as the classifier of choice when it comes to this project. Multiple IoT devices nowadays hold Computer Vision CNN-based nets capable of much more, speaking to the potential of this technology.

## Conclusion and bibliography:

1. **Data Utilization and Preprocessing:** The research emphasizes the importance of the sequential nature of sEMG signals, employing a sliding window technique to segment the data effectively.

2. **Model Architecture and Training:** The CNN-based model was selected for its robustness in handling spatial and temporal dependencies inherent in sEMG data. Feature extraction and augmentation played a significant role in improving classification performance, as these steps allowed the model to focus on critical patterns within the data.

3. **Performance and Evaluation:** Although the model achieved commendable accuracy, certain challenges remained, particularly in distinguishing movements with similar muscle activation patterns.



4. **Challenges and Future Directions:** The transition to a feature-based approach highlighted several challenges, notably the need for further optimization to enhance the model's robustness against noise and variability in the signals.

5. **Innovative Approaches:** The introduction of an additional variable set to improve the model's robustness against noise is a novel approach that merits further exploration.

## Practical Implications

The findings from this research have significant implications for the development of assistive technologies, particularly in the field of prosthesis and rehabilitation. Accurate classification of hand and wrist movements using sEMG signals can lead to more intuitive and responsive control systems for prosthetic limbs. The advancements in feature extraction and model training presented in this thesis contribute to the growing body of knowledge aimed at improving the quality of life for individuals relying on assistive devices.

Additionally, as the scope for a future collaboration between UHG and Comillas ICAI broadens, this POC has proven fruitful to determine the initial approach to this technology and the tests to be performed.

## Future Work

While this project was definitely a POC for a bigger scope, it still manages to light up some areas that can have a profound impact in research. Thus, next steps from this POC can be easily determined.

1. **Power consumption and heat dissipation:** Optimizing power efficiency and thermal management is critical for implantable devices that require long usage hours and high computational loads.
2. **Telemetry and wireless communications:** Enabling wireless data transmission is essential for seamless telemetry and remote device management without invasive procedures.
3. **Digital pre-processing:** Integrating digital preprocessing on the implant's microprocessor can reduce data transmission overhead and enable more efficient, real-time signal analysis.



*A Santi, por la valentía que me brinda.  
A Violetita, por la alegría que despierta.  
A Nuka, por la fuerza que me infunde.*

*Nothing ever comes that  
is not the fruit of your work.*



# Contents

|          |  |           |
|----------|--|-----------|
| <b>1</b> | <b>Context of the Project, Design and testing of a Human-Machine Interface</b>             | <b>1</b>  |
| 1.1      | A brief explanation of trauma in nerves and locomotion. Characterizing Neuroma. . . . .    | 2         |
| 1.2      | sEMG for muscle activation characterization . . . . .                                      | 3         |
| 1.3      | HMI Interfacing Design . . . . .   | 5         |
| 1.4      | Designing a Hardware EMG-recorder device. . . . .  | 5         |
| 1.4.1    | Amplification phase: . . . . .   | 8         |
| 1.4.2    | Filtering phase: . . . . .   | 9         |
| 1.4.3    | ADC and capturing: . . . . .   | 9         |
| 1.5      | Clinical Trials, Learnings and Results . . . . .   | 14        |
| <b>2</b> | <b>Classifying the behaviour of EMG in trans-humeral amputees through DL applications.</b> | <b>19</b> |
| 2.1      | Methodology . . . . .  | 20        |
| 2.1.1    | Recurrent Neural Networks (RNN) . . . . .  | 20        |
| 2.1.2    | Long Short-Term Memory (LSTM) Networks . . . . .   | 21        |
| 2.1.3    | Gated Recurrent Units (GRUs) . . . . .   | 21        |
| 2.1.4    | Comparison of RNNs, LSTMs, and GRUs for EMG Classification . . . . .                       | 22        |
| 2.1.5    | CNN and CNN in sEMG . . . . .  | 23        |
| 2.1.6    | Dataset Explanation . . . . .  | 24        |
| 2.1.7    | Features . . . . .   | 25        |
| 2.1.8    | Model Architecture . . . . .   | 26        |
| 2.1.9    | Training procedure . . . . .   | 29        |
| 2.2      | Experiments . . . . .  | 31        |
| 2.2.1    | Experiment A: . . . . .  | 31        |
| 2.2.2    | Experiment B: . . . . .  | 32        |
| 2.2.3    | Experiment C: . . . . .  | 33        |

|  |           |
|--|-----------|
| <b>3 Conclusion and Future steps</b>           | <b>37</b> |
| 3.1 Conclusion . . . . .                       | 37        |
| 3.1.1 Key Findings and Contributions . . . . . | 37        |
| 3.1.2 Practical Implications . . . . .         | 38        |
| 3.2 Future Work . . . . .                      | 38        |
| 3.3 Conclusion . . . . .                       | 40        |
| <br>   |           |
| <b>Appendix</b>                                | <b>41</b> |
| <br>   |           |
| <b>A Planos de Diseño</b>                      | <b>41</b> |
| <br>   |           |
| <b>B Ethical Compliance</b>                    | <b>43</b> |
| <br>   |           |
| <b>C Sustainable Development Goals</b>         | <b>45</b> |
| <br>   |           |
| <b>Bibliografía</b>                            | <b>47</b> |

# List of Figures

|     |  |    |
|-----|--|----|
| 1   | Aspecto final de la parte de grabación analógica del dispositivo de grabación sEMG diseñado en este proyecto. . . . .  | iv |
| 2   | Plano de la fase de amplificación. Muestra una fase de amplificación analógica de sEMG de dos canales. Se tomó la decisión de diseño de incluir dos canales de grabación para aprovechar al máximo la capacidad de doble canal del ADALM-2000. . . . .   | v  |
| 3   | Final look of the Analog Recording part of the prototype sEMG recording device designed in this project. . . . .   | x  |
| 4   | Amplification phase blueprint. It shows a two channel sEMG analog amplifying phase. A choice was made during the design two include two recording channels to make full use of the ADALM-2000 double channel capacity. . . . .   | xi |
| 1.1 | Explanatory graph of a single neuron action-potential generation. From [2] . . . . .   | 3  |
| 1.2 | Representation of a SMU (Single Motor unit) from The origin of bio potentials - Scientific Figure on ResearchGate. [5] [accessed 2 Jun, 2024] . . . . .  | 4  |
| 1.3 | The image shows <b>three examples of electromyogram (EMG) recordings</b> from individuals with different neuromuscular conditions. 1) 44 year old Male without neuromuscular condition history. 2) 62 year old man with chronic low back pain and neuropathy. 3) 57 year old man with myopathy . . . . . | 6  |
| 1.4 | Amplification phase of the Analog EMG section of the EMG recorder device. AD8422 is a rail-2-rail instrumentation amplifier that provides robust input protection without sacrificing noise performance. . . . .   | 8  |
| 1.5 | pin-out diagram for the AD8422 rail to rail instrumental amplifier. Courtesy of Analog Devices. . . . .  | 9  |

|      |   |    |
|------|---|----|
| 1.6  | Filtering phase of the Analog EMG section of the EMG recorder device. It is comprised of two amplifiers in a non-inverting configuration, the shown configuration provides a low-pass filter with a cut-off frequency of 10kHz (-3dB gain at 10kHz). . . . .  | 10 |
| 1.7  | Simulation plot from a filtering phase LTSpice simulation. The green plot shows the voltage of a 10kHz sine wave at the beginning of the filtering and the blue shows its corresponding dampened signal. Since 10kHz is the cut-off frequency there is a dampening of 3dB and a slight delay of $90^\circ$ . . . . .                                      | 10 |
| 1.8  | ADALM2000 Active Learning Module Portable Oscilloscope by Analog Devices . . . . .  | 11 |
| 1.9  | Amplification phase blueprint. It shows a two channel sEMG analog amplifying phase. A choice was made during the design two include two recording channels to make full use of the ADALM2000 double channel capacity. . . . .   | 12 |
| 1.10 | Filtering phase with two channels. . . . .  | 12 |
| 1.11 | Snapshot of the final prototype PCB design in kiCAD PCB editor. . . . .   | 13 |
| 1.12 | Final Printed PCB as shown during the tesbench performed in the lab to test it's performance. . . . .   | 13 |
| 1.13 | Photography during the workshops at UHG to understad the core of the problem and get to know the team under Dr.Andrés Maldonado . . . . .   | 14 |
| 1.14 | Test-bench with one of the rabbit subjects to test the electrodes and show the behaviour of the muscle tissue. . . . .  | 15 |
| 1.15 | Image from the Environmental Lab at university taken during the sealing operation of the bio-compatible casing. Using UV,the same resin used in the Additive Manufacturing process, is cured to seal the prototype. . . . .   | 16 |
| 1.16 | Image of the operating room during the subcutaneous implantation of the advanced device . . . . .   | 17 |
| 1.17 | Image taken post-operation where the testing process can be seeing taking place. The rabbit is encased in a box, while at the same time monitoring the prototype through the explained interfacing (Scopy and ADC). The image shows the instant activation is recorded for the first time from the EMG capturing device implented on the subject. . . . . | 18 |
| 2.1  | Structure of an LSTM neuron. Image taken from Liu et al. (2020). . . . .  | 21 |
| 2.2  | Simple LSTM model architecture . . . . .  | 26 |
| 2.3  | Simple GRU model architecture . . . . .   | 27 |
| 2.4  | Simple Bidirectional model architecture . . . . .   | 27 |
| 2.5  | Double Layer CNN model for classification . . . . .   | 28 |



- 2.6 Snippet of part of the resulting dataset when the model overfitted to the average mean value of the multiclass output. . . . . 30
- 2.7 Results showing a snippet of the test set and classification via the three simple models over two labels . . . . . 32
- 2.8 ROC curve with AUC values for the binary classification of each multiclass label . . . . . 34



# List of Tables

|     |  |     |
|-----|--|-----|
| 1   | Resultados de la prueba del experimento C en la clasificación de 6 etiquetas . . . . .   | vi  |
| 2   | Test results of experiment C on 6 label classification . . . . .   | xii |
| 2.1 | Table showing the encoded labels used in this paper for training the model belonging to datasets NINAPRO DB3 and DB5 . . . . . | 25  |
| 2.2 | sEMG Signal Features and formulas . . . . .  | 26  |
| 2.3 | Architecture information of the training platform . . . . .  | 29  |
| 2.4 | Experiment A <b>training</b> results across all 3 simple models, LSTM, GRU and Bidirectional. . . . .                          | 31  |
| 2.5 | Experiment A <b>testing</b> results across all 3 simple models, LSTM, GRU and Bidirectional. . . . .                           | 32  |
| 2.6 | Train results of experiment B . . . . .  | 33  |
| 2.7 | Test results of experiment B . . . . .   | 33  |
| 2.8 | Test results of experiment C on 6 label classification . . . . .   | 34  |
| 2.9 | AUC for every label in Experiment C . . . . .  | 34  |



# Acrónimos

|             |  |
|-------------|--|
| <i>ICAI</i> | Instituto Católico de Artes e Industrias |
| <i>FMT</i>  | Final Master Thesis                      |
| <i>sEMG</i> | Surface Electro-Miography                |
| <i>CNS</i>  | Central Nervous System                   |
| <i>SNR</i>  | Signal to Noise Ration                   |
| <i>PCB</i>  | Printed Circuit Board                    |
| <i>RNN</i>  | Recurrent Neural Network                 |
| <i>LSTM</i> | "Long-Short Term" Memory neural network  |



# Chapter 1

## Context of the Project, Design and testing of a Human-Machine Interface

In this initial chapter of the thesis the original overarching project surrounding this thesis will be presented and the part from which this research avenue stems explained.

**This project complies with the ethical guidelines stated by UHG ethical board as seen in the ethical annex.**

The core of this project derives from a collaboration that took place between the University Hospital of Getafe "peripheral nerve and brachial plexus unit" and the electronics and automations department at Comillas ICAI. In these regard the leading coordinator of this unit at UHG, Dr.Andrés A. Maldonado and his team contacted Prof. Romano Gianetti for help developing a POC for a device capable of measuring sEMG in order to control prosthetic limb. When i joined the team a visit to this hospital and the facilities was scheduled where the root of the problem was explained and coordination on this project started on both ends.

The collaboration was staged to begin with the design of an electronic prototype of a sEMG recorder. Comprised of an amplification and cleanup analog phase. Once this prototype had been built, an operation would happen where the mentioned surgeons would interface this device with a couple of electrodes inplanted on a traumatised limb of a rabbit for testing. After success in this regard the project would move on further into prototyping and testing in humans.

The scope of my FMT is tangential to this project in that the design, and rapid prototyping of the HW platform aforementioned is within the scope of my work, but after that the goal is to study sEMG behaviour and determine the key markers that can help us understand neural behaviour on traumatised neural pathways. e.g the ones found on these type of limbs. Thus the project takes both electronics and

signal processing, as well as a ML and DL approach to the issue.

In order to further understand the needs for this research it is important to explain even though briefly the neurological and physiological side of the issue.

## 1.1 A brief explanation of trauma in nerves and locomotion. Characterizing Neuroma.

Accidents that involve any type of violent force to limbs and the human body can lead to, sometimes fatal, and often traumatic injuries to the human body. Due to their location and exposure as extremities, the limbs of the human body are often the affected party in these exchanges. The Peripheral Nervous System (PNS) of the human body is often overlooked in the aftermath, when a traumatising injury befalls a limb. The PNS is comprised of all the nerves of the human body that branch out from the CNS and is further subdivided into *somatic and autonomic nervous system*.

Connecting the PNS from the CNS to the rest of the body, in a amputation case trauma shall befall the nervous ends in charge of gathering information and controlling the muscle tissue of the amputated limb. These *motor end plates* after a cut become a traumatised neural end. Nowadays multiple procedures appear in the literature and are starting to be performed aiming to save as much of these neural ends as possible and guarantee a potential use on prosthetic development in the future. For the purpose of these research we are going to assume the opposite state where a nerve is amputated or cut violently. Afterwards healing will happen to these injured neural pathways along with the surrounding tissue to create what is commonly referred to as a stump. Inside this limb ending, the tangled mess of neural ends is called a *Neuroma*[10].

A healthy neuron has a resting membrane potential of around -70 mV, maintained by differences in ion concentrations (mainly Na<sup>+</sup>, K<sup>+</sup>, Cl<sup>-</sup>) inside and outside the cell, and by the action of the sodium-potassium pump. When a neuron receives sufficient exciting input (e.g., from neurotransmitters binding to receptors), its membrane potential depolarizes. If this depolarization reaches a threshold (usually around -55 mV), an action potential is triggered. The rising phase of the action potential is caused by the opening of voltage-gated sodium (Na<sup>+</sup>) channels. Na<sup>+</sup> rushes into the cell, further depolarizing the membrane potential to around +40 mV. The falling phase is caused by inactivation of Na<sup>+</sup> channels and opening of voltage-gated potassium (K<sup>+</sup>) channels. K<sup>+</sup> exits the cell, repolarizing the membrane back towards the resting potential. After the spike, the membrane briefly hyperpolarizes due to continued K<sup>+</sup> efflux, before returning to the resting state. The action potential propagates along the axon as the depolarization spreads,



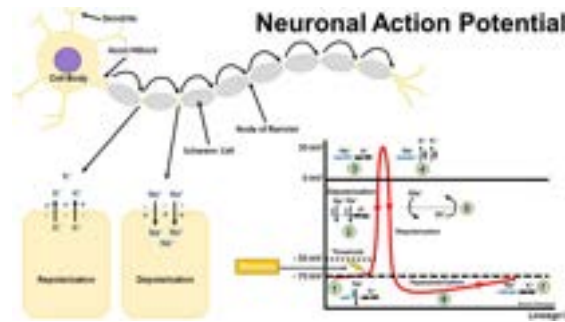


Figure 1.1: Explanatory graph of a single neuron action-potential generation. From [2]

sequentially opening adjacent voltage-gated channels. This allows the signal to travel long distances without decrement. In myelinated axons, action potentials jump between the nodes of Ranvier (gaps in the myelin sheath) in a process called "*saltatory conduction*", allowing faster propagation. Action potentials are "all-or-none" events that occur in a stereotyped way when the threshold is reached. Their amplitude and shape are independent of the strength of the triggering stimulus. After an action potential, there is a brief refractory period during which a new action potential cannot be initiated, ensuring unidirectional propagation

## 1.2 sEMG for muscle activation characterization

In traumatic neuroma, the injured axons can show abnormal electro-physiological activity, like spontaneous discharges and mechanical hypersensitivity. The disorganized regrowth of axons likely leads to erratic and abnormal motor neuron potentials. [4]. As such characterization of these signals can lead to misleading results. On the other hand, sEMG are the signals generated by the muscle fibers during contraction that can be measured on the skin surface over the muscle.

This signal is the amalgamation of multiple electrical activities across many motor units. The depolarization that happens in a Neuron is transmitted into the neuro-muscular junction which is the point where a neuron and a motor cell join. This group of cells, both neurons and the corresponding innervated muscle cells connected, are called a single motor unit or SMU 1.2. The action potential then transmits from those muscle fibers across the muscle in a range of frequencies of 20-500 Hz. As a general approach to understanding the potential of control between a trauma and a prosthesis, the choice of sEMG came down to the following principles:

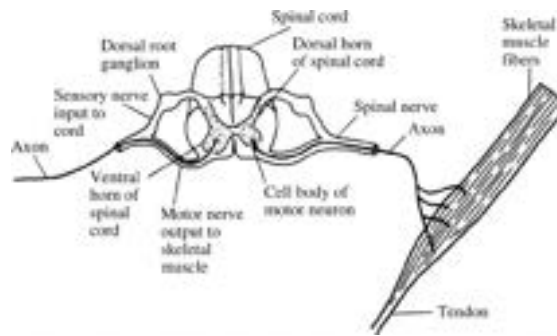


Figure 1.2: Representation of a SMU (Single Motor unit) from The origin of bio potentials - Scientific Figure on ResearchGate. [5] [accessed 2 Jun, 2024]

1. **Ease of use:** sEMG is non-invasive, while iEMG requires inserting needle electrodes into the muscle. For a painful condition like a neuroma, the non-invasive nature of sEMG is advantageous to avoid causing additional pain or discomfort to the patient. sEMG is easier to apply in a clinical setting, as it does not require the same level of expertise and precision as iEMG for electrode placement. This makes it more practical for routine assessments of patients with neuroma.
2. **Explained behaviour:** sEMG provides a more global measure of muscle activity, as the electrodes record from a larger area on the skin surface. This can be useful in assessing overall muscle function and activation patterns related to the neuroma. In contrast, iEMG is more localized and records from a smaller area within the muscle. While this can provide detailed information about individual motor units, it may miss the bigger picture of how the muscle is functioning as a whole in relation to the neuroma.
3. **Previous Literature:** sEMG has been shown to have good sensitivity and specificity for distinguishing between healthy individuals and those with various neuromuscular conditions, suggesting it could be a useful tool for evaluating the goals of this project.

In summary, the non-invasive, global, and clinically accessible nature of sEMG, along with its proven utility in assessing neuromuscular function, make it a preferred choice over iEMG for evaluating patients with neuromas in many cases. However, the specific clinical question and individual patient factors would ultimately guide the choice between these techniques.

## 1.3 HMI Interfacing Design

The core of the project stems from the briefly mentioned collaboration between the University Hospital of Getafe "peripheral nerve and brachial plexus unit" and the electronics and automation's department at Comillas ICAI. In this chapter we will explain in detail the original project, the design and manufacture of the original prototype for the analog sEMG capture device envisioned. Also at the end, the evolution of that original prototype into a digital capture device completely manufactured will be explained briefly.

As a disclaimer for this chapter and subsequent ones, some graphic images from operations with animals and use of the prototypes will be shown.

## 1.4 Designing a Hardware EMG-recorder device.

The nature of sEMG and other bio-signals stem from the use of the human body of electric and chemical means of communication. As mentioned in previous chapters this signals are called Action Potentials and are at the very core a discharged caused by the polarization-depolarization of membranes. The figure 1.3 shows examples of EMG recordings that perfectly illustrate the main points that need to be addressed for the design of our EMG-recorder device.

1. **Maximizing the signal-to-noise ratio:** The EMG signal is very small (0-10 mV peak-to-peak or 0-1.5 mV RMS) compared to potential noise sources. Key noise sources include inherent noise from electronic components, ambient electromagnetic noise (e.g. 50/60 Hz from power lines), motion artifacts from electrodes and cables, and interference from other bio-potentials like ECG. Using high quality electronics, proper circuit design and construction techniques is important to maximize the signal-to-noise ratio.
2. **Avoiding distortion of the EMG signal:** The relative contribution of different frequency components in the EMG signal should not be altered by the recording process. The EMG signal has usable energy from 0-500 Hz, with dominant energy between 50-150 Hz. Filters used to reduce noise must be designed carefully. Distortion due to delay is unavoidable. Furthermore, this delay is dependant due to the nature of non-linear amplification on the frequency, meaning a "waveform distortion" will appear with different levels of phase being applied on different harmonics. There will be a need for precisely determining the operating frequency band.
3. **Selecting appropriate electrodes** for the application: Surface electrodes are non-invasive but have limitations - they can only record superficial mus-

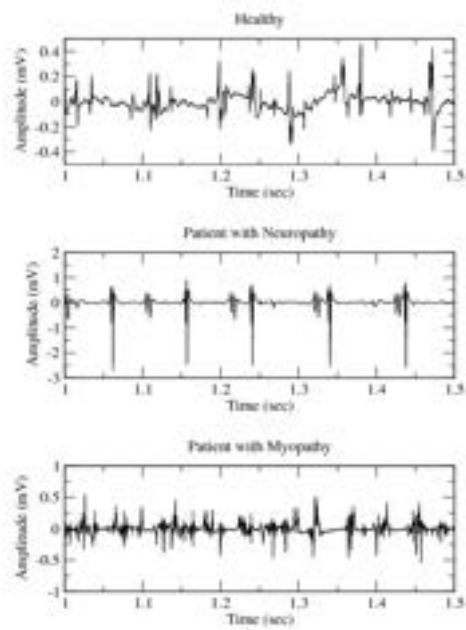


Figure 1.3: The image shows **three examples of electromyogram (EMG) recordings** from individuals with different neuromuscular conditions. 1) 44 year old Male without neuromuscular condition history. 2) 62 year old man with chronic low back pain and neuropathy. 3) 57 year old man with myopathy

cles, are affected by subcutaneous tissue, and risk cross-talk from adjacent muscles. Intramuscular fine-wire or needle electrodes can record from deep muscles and specific motor units but are invasive. Electrode material, size, shape and inter-electrode distance affect selectivity and signal quality. The choice of surface or intramuscular electrodes depends on the specific clinical or research application. [6]

On the issue of appropriate electrodes the University Hospital of Getafe has kindly lent the project a set of electrode pairs that will be used to test and prototype during the design phase while the most advanced or even more invasive ones will be saved for the trials. As such we will be mentioning their models and characteristics as they begin appearing along the project.

Given all of this conditions the design choice relied mainly now on the way this different challenges will be tackled. There is a wide array of electronics capable of filtering, whether digital or analog, and cleaning the signal as intended but each one offers it's own set of challenges. The nature of this thesis compelled the design to follow a more analog approach. With an analog circuit with a pass band filter and a rudimentary but effective amplification we can tackle the issue of cleaning up the unwanted noise outside of our main operational frequency band (up to 10kHz), while avoiding the need for programming a filter/amplifier after the ADC. In this case 10kHz is not a significant enough cutoff frequency to induce much latency and/or quantization error. But the option for a simple amplifying and filtering circuit proved to be reliable for our purposes. After this analog stage a portable oscilloscope model ADALM-2000 will be employed to capture the signal and then capture it and visualise it on a computer.

The analog circuit itself is comprised of 2 sections: an **amplifying phase and a filtering phase**. Also the analog circuit is a floating differential EMG recording device. The nature of a signal in the human body is that we cannot rely on a ground connection and the differential EMG recording device would provide us a comprehensive recording of the SMU action potentials happening across the muscle. Thus, deep care was also put on reducing incoming noise from power sources and from floating voltages.

The amplifying phase's main goal is to increase the definition of the incoming signal without affecting the SNR. If filtering happened first, it would attenuate parts of the signal close to the noise floor, and then amplifying would boost noise as much as signal, resulting in poor SNR. This way the second phase, filtering, can reliably cut more of the noise out of the wanted EMG. The different sections of the circuit can be seeing in the following figures

The power sources and the sources of the amplifier have been lined with graphite beads and condensers to reduce the source-noise.

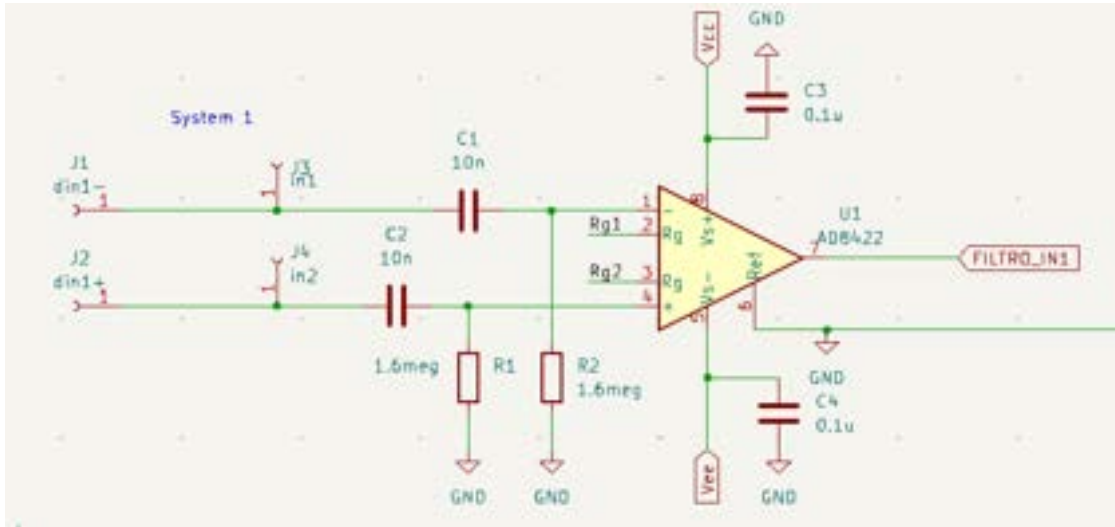


Figure 1.4: Amplification phase of the Analog EMG section of the EMG recorder device. AD8422 is a rail-2-rail instrumentation amplifier that provides robust input protection without sacrificing noise performance.

### 1.4.1 Amplification phase:

The instrumental amplifier proved to be a reliable choice to base the amplification phase upon. There are 3 main features why we choose this model:

1. **Low-power consumption:** aiming at a future wearable device to control a prostheses we need to take into account power consumption even at early stages of the process. The AD8422 has a maximum quiescent current of only  $368 \mu\text{A}$ , making it well-suited for power-sensitive applications.
2. **Low noise and distortion:** With a maximum input voltage noise of  $8 \text{ nV/Hz}$  at  $1 \text{ kHz}$  and  $0.15 \mu\text{V}$  p-p RTI noise (at gain of 100), the AD8422 is a low-noise amplifier. It also achieves low distortion, with  $0.5 \text{ ppm}$  non-linearity at a gain of 1 with a  $2 \text{ k}\Omega$  load. For us SNR is critical and given that the frequency band we will be operating with ranges from 0 to  $10 \text{ kHz}$  then it suits the requirements properly.
3. **Adjustable gain:** The gain the device has can be adjusted by a external set of resistors. This would prove useful as setting up multiple gains can help testing and counteracting the auto-focus setting on the capturing device.

To modify the gain value of the amplification circuit, the manufacturer provides in the spreadsheet the following formula:

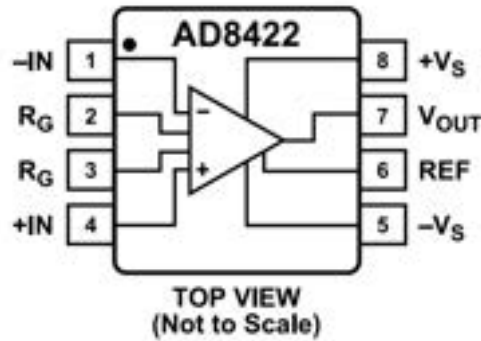


Figure 1.5: pin-out diagram for the AD8422 rail to rail instrumental amplifier. Courtesy of Analog Devices.

$$G = 1 + 19.8k\Omega/R_G$$

Where  $G$ , corresponds to the wanted Gain value and  $R_g$  to the variable resistance that is added externally per the figure 1.5.

Further considerations have been taken to reduce unwanted noise from sources or other artifacts to appear in our signal, such as graphite beads to  $V_{cc}$  and  $V_{ee}$  and a high-pass filter to take out any offset coming in from the measurement.

### 1.4.2 Filtering phase:

The subsequent filtering phase main goal is to maximise SNR. In order to do this a low pass filter implementation will occur where the frequency cut-off will happen at 10kHz. Given that sEMG and EMG signals frequency band lies between 0 and 10kHz, more concentrated around 1kHz, the design took the shape of the 1.6 The image in 1.7 shows the plot simulated and expected at 10kHz for the filtering circuit.

The filtering phase can phase the signal up to  $90^\circ$  from the original one. This has been deemed enough for our uses. The lower the frequency the bigger the delay the signal suffers, but since the signal is focused around the bands for 1kHz and around, then the average delay would be around 0,25 ms. Which can be disregarded for our current prototyping.

### 1.4.3 ADC and capturing:

An HMI is characterized for translating biomedical signals to digital ones. The amplification and filtering were performed in Analog so the use of an ADC is

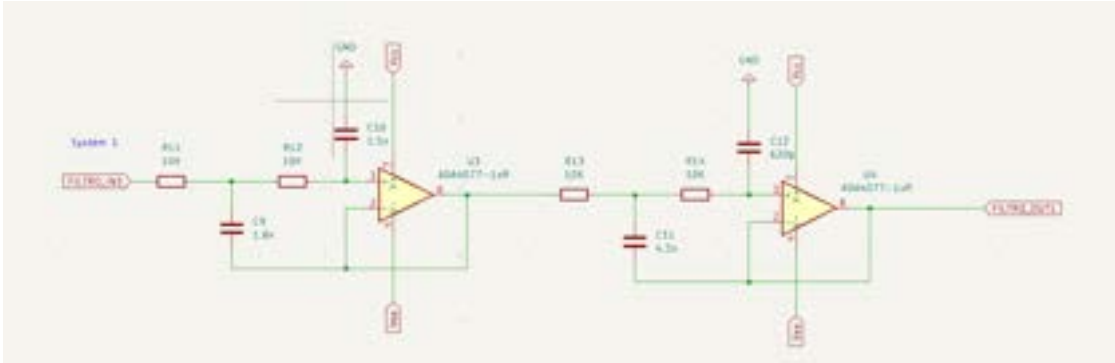


Figure 1.6: Filtering phase of the Analog EMG section of the EMG recorder device. It is comprised of two amplifiers in a non-inverting configuration, the shown configuration provides a low-pass filter with a cut-off frequency of 10kHz (-3dB gain at 10kHz).

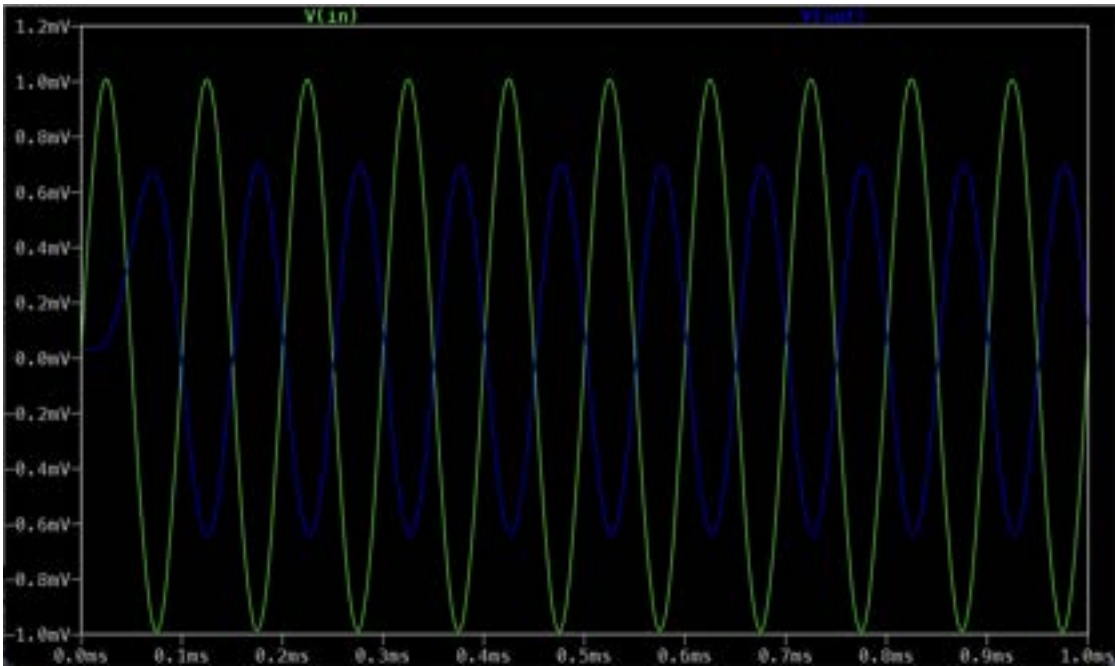


Figure 1.7: Simulation plot from a filtering phase LTSpice simulation. The green plot shows the voltage of a 10kHz sine wave at the beginning of the filtering and the blue shows its corresponding dampened signal. Since 10kHz is the cut-off frequency there is a dampening of 3dB and a slight delay of  $90^\circ$ .





Figure 1.8: ADALM2000 Active Learning Module Portable Oscilloscope by Analog Devices

needed to finalize the EMG capture device. With the use of ADALM2000 Active Learning Module to sample the signal and the Scopy program to visualize it we finalized our prototype. This tool by Analog Devices belongs to a family of portable oscilloscopes. This device would prove useful for the following reasons:

- **High sampling rate and resolution:** The ADALM2000 features 12-bit ADCs running at 100 MSPS. This allows it to accurately digitize signals up to 25 MHz bandwidth. The high sampling rate and resolution are important for capturing cleaned up analog signals with minimal loss of information.
- **Compact and affordable:** The ADALM2000 integrates the ADC and many other instruments into a small, portable form factor that can fit in a pocket. And it does this at a very affordable price point compared to standalone benchtop instruments. This makes it an economical choice for digitizing signals in a variety of settings, like laboratory or hospital.
- **Sufficient analog bandwidth:** While the ADC runs at 100 MSPS, the analog input bandwidth is around 25-30 MHz. This is more than enough for most applications, allowing the ADC to faithfully capture the full spectrum of the cleaned up analog signal without aliasing.

The design of the analog phase - amplification and filtering - thus had to be adapted to fit the multiple range of electrodes used and also the connection to the ADALM ADC phase. For manufacturing the tool kiCad was employed to adapt the electronic design into a PCB design. Then a BOM was generated and the PCB printed. The choice of components was made with cost and PCB real-state in mind, as well as the requirements of the design.

For more details refer to the Annexes where the full electronic and PCB blueprints will be attached.

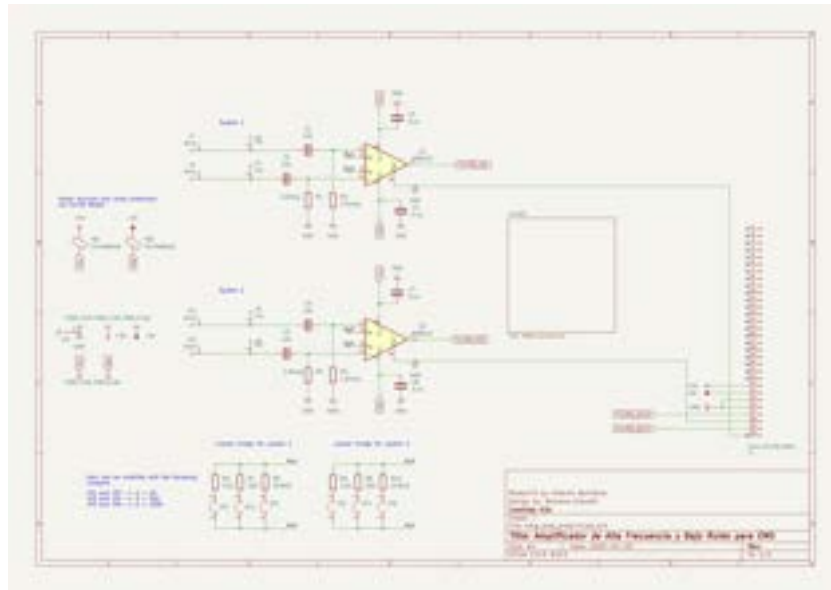


Figure 1.9: Amplification phase blueprint. It shows a two channel sEMG analog amplifying phase. A choice was made during the design two include two recording channels to make full use of the ADALM2000 double channel capacity.

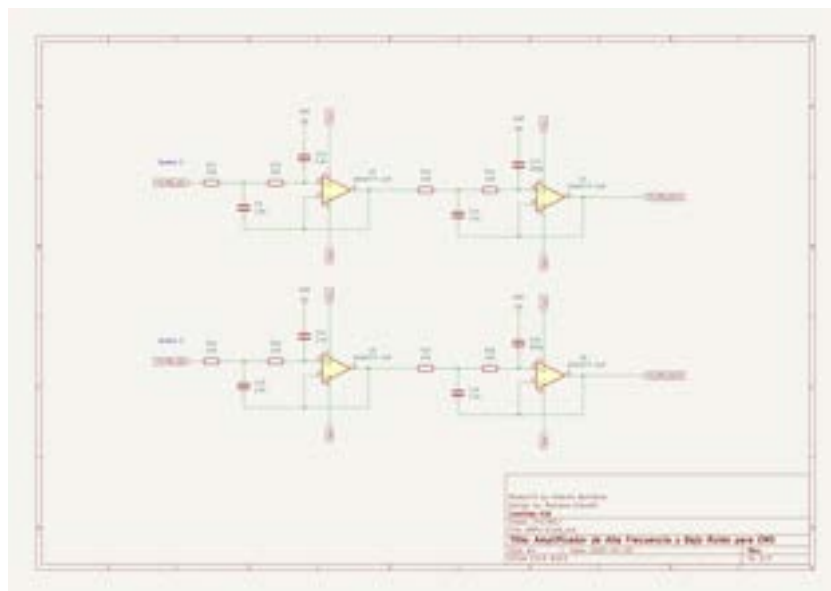


Figure 1.10: Filtering phase with two channels.

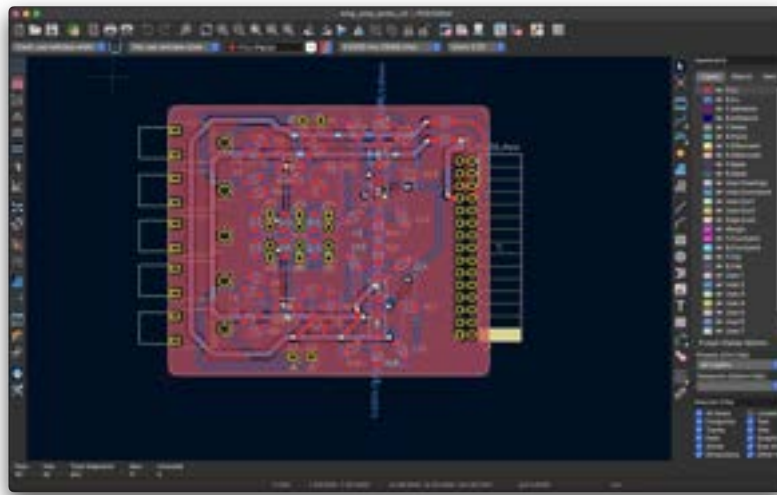


Figure 1.11: Snapshot of the final prototype PCB design in kiCAD PCB editor.



Figure 1.12: Final Printed PCB as shown during the tesbench performed in the lab to test it's performance.



Figure 1.13: Photography during the workshops at UHG to understand the core of the problem and get to know the team under Dr. Andrés Maldonado

## 1.5 Clinical Trials, Learnings and Results

Being the main goal of this collaboration the use of the prototype in a clinical environment a series of tests and trials have been performed with Dr. Andrés Maldonado and his team to test the viability of the prototype throughout various clinical trials.

Originally Prof. Romano Gianetti, Prof. Jose Daniel Muñoz Frias and two students, Alvaro Martín and me, attended the hospital of Getafe to an introduction to the topic on February 2023. Then a phase of State of the Art was kicked off until September 2023 when the design phase of the prototype started. In the meanwhile a series of trials took place to determine the best way to insert the device. The trial subjects came from a supply of testing rabbits owned by the Hospital for such tests. At first the design consisted in protruding cables connected to electrodes embedded in the muscle tissue. This way proved to be dangerous to the rabbits we performed trials with, due to the damage and loss of blood that could occur when the rabbit tried to extract the cables from its hind legs, where the electrodes were implanted for testing. Another lesson learned from the original test came from



Figure 1.14: Test-bench with one of the rabbit subjects to test the electrodes and show the behaviour of the muscle tissue.

the muscle tissue itself. As explained at the beginning of this chapter, a Neuroma is a amalgam of muscle and neural tissue, and although it behaves slightly different than existing tissue, it still needs blood flow to generate biomedical signals.

Subsequent attempts focused on subcutaneous implantation of the full device in a biocompatible casing and transmitting the signal via bluetooth. As such, a new device was designed on the basis of the prototype that is the topic of this thesis. This advanced implantable was requested, designed and built by a third party.

The testing of the prototype, as well as the trials with the advanced piece were succesful in highlighting the viability of this process to capture EMG signals from muscle tissue.

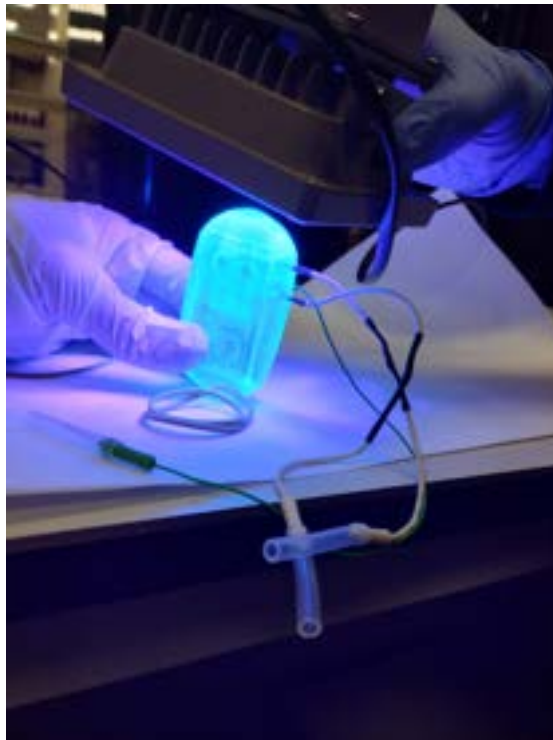


Figure 1.15: Image from the Environmental Lab at university taken during the sealing operation of the bio-compatible casing. Using UV, the same resin used in the Additive Manufacturing process, is cured to seal the prototype.



Figure 1.16: Image of the operating room during the subcutaneous implantation of the advanced device



Figure 1.17: Image taken post-operation where the testing process can be seen taking place. The rabbit is encased in a box, while at the same time monitoring the prototype through the explained interfacing (Scopy and ADC). The image shows the instant that activation is recorded for the first time from the EMG capturing device. 18



## Chapter 2

# Classifying the behaviour of EMG in trans-humeral amputees through DL applications.

The particular application for this project will guarantee the ability for amputees and people suffering from traumatic injuries to not be limited in movement via the application of the discoveries from the previous chapter 1. Nevertheless, as explained, Neuroma pose a significant issue when analysis are performed due to the special and often traumatic nature of their appearance. The signal itself will experience changes in it's shape meaning shifting properties both in the time-domain and frequency-domain. To showcase this and try to classify the behaviour of these signals a study will be performed applying DL techniques with a publicly available dataset of sEMG signals.

EMG signals are bio-electric action-potentials that propagate across the muscular tissue. These bio-signals have many properties in the time domain and in the frequency domain that are popularly used to extract bio-markers of health and behaviour - e.g. tissue deterioration from shifts in frequency range - for the respective muscle behind. Continuing the work in the MEng Thesis titled *Embedded Sensorization and Deep Learning Based Classification for Prosthetic Control* [7], this paper aims to provide a exhaustive understanding of EMG in Neuroma - traumatised muscle tissue - for the purpose of the overarching research proposed in the paper aforementioned [7] .

This paper includes an explanation on the dataset employed for the analysis - NinaPro MeganePro Dataset -, as well as explanations of the methodology used, the DL models employed (LSTM, RNN, GRU, ...) and other tools. The final classification results will be compared against a test-bench of popular models from [1] [8]

## 2.1 Methodology

Before explaining the experiment and the methodology it is important to understand the tools employed. The main goal of this is to create a classifier through which we can understand how to approach the problem at hand.

The past few decades have witnessed unprecedented advancements in the field of deep learning (DL), transforming how we approach and solve complex problems across various domains. Initially driven by the resurgence of neural networks and the development of sophisticated architectures, DL has become the cornerstone of modern artificial intelligence (AI) systems. With the advent of powerful computational resources and large-scale datasets, neural networks have evolved from simple perceptron models to intricate architectures capable of learning from vast amounts of data. Convolutional Neural Networks (CNNs) revolutionized image recognition, while advancements in Recurrent Neural Networks (RNNs) have significantly impacted sequential data processing, such as natural language processing and time-series analysis.

### 2.1.1 Recurrent Neural Networks (RNN)

Recurrent Neural Networks (RNNs) represent a class of neural networks that are particularly well-suited for processing and analyzing sequential data, such as time-series. Unlike traditional feedforward neural networks, RNNs possess recurrent connections that enable them to maintain an internal state or "memory." This capability allows RNNs to capture and utilize temporal dependencies in the input data, making them ideal for applications where contextual information across time steps is crucial such as signals of any kind. Predominant applications include sound-related signal processing. Applying the same principles we can utilize this family of NN to our advantage in the time domain of the sEMG.

In a standard RNN, the output from a neuron can be fed back as input to neurons in the previous layers. At each time step, the RNN receives an input and produces an output based on the current input and the internal state derived from previous time steps. This recurrent feedback loop facilitates the persistence of contextual information, allowing the network to learn complex temporal patterns. However, vanilla RNNs face significant challenges due to the vanishing and exploding gradient problem, which limits their ability to learn long-term dependencies effectively.

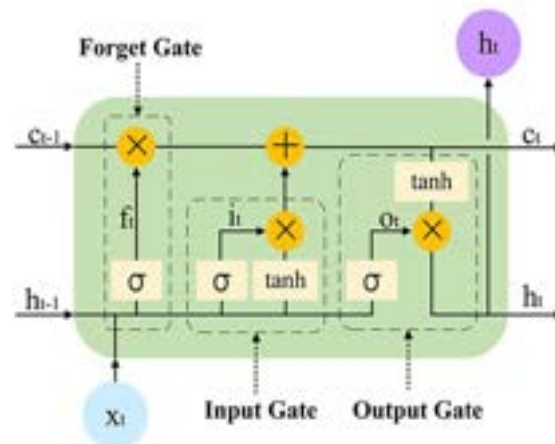


Figure 2.1: Structure of an LSTM neuron. Image taken from Liu et al. (2020).

## 2.1.2 Long Short-Term Memory (LSTM) Networks

To address the limitations of vanilla RNNs, Long Short-Term Memory (LSTM) networks were developed. LSTMs extend the capabilities of RNNs by introducing a "memory cell," a specialized unit designed to maintain its state over extended periods. The memory cell is regulated by three distinct gates: the forget gate, the input gate, and the output gate.

- Forget Gate: Determines what information should be discarded from the cell state.
- Input Gate: Decides what new information should be stored in the cell state.
- Output Gate: Controls what information is output based on the current input and the cell state.

At each time step, the LSTM can selectively read from, write to, or reset the memory cell using these gates. This sophisticated gating mechanism allows LSTMs to learn and capture both short-term and long-term dependencies, making them particularly effective for tasks involving sequential data, such as Electromyography (EMG) signal classification.

## 2.1.3 Gated Recurrent Units (GRUs)

Gated Recurrent Units (GRUs) represent a more recent advancement in RNN architectures, aiming to address the vanishing gradient problem with a simpler design compared to LSTMs. GRUs combine the forget and input gates into a single

"update gate" and merge the cell state and hidden state. This streamlined structure reduces the computational complexity while retaining the ability to capture long-term dependencies.

- Update Gate: Controls how much of the previous memory to retain.
- Reset Gate: Determines how to combine the new input with the previous memory.

The simpler architecture of GRUs results in faster training times and lower computational requirements, often achieving comparable performance to LSTMs in various applications.

#### 2.1.4 Comparison of RNNs, LSTMs, and GRUs for EMG Classification

In the realm of Electromyography (EMG)-based gesture recognition, a variety of studies have been conducted to evaluate and compare the performance of Recurrent Neural Networks (RNNs), Long Short-Term Memory networks (LSTMs), and Gated Recurrent Units (GRUs). These studies highlight both the strengths and limitations of each architecture, offering insights into their suitability for surface EMG (sEMG) classification models.

##### **Simão et al**

. Simão et al. conducted a comprehensive comparison between vanilla RNNs, LSTMs, and GRUs, focusing on their classification accuracies and computational efficiencies. The key findings from this study revealed that although vanilla RNNs, LSTMs, and GRUs achieved similar levels of classification accuracy, LSTMs and GRUs had a distinct advantage in terms of model complexity and computational efficiency. Specifically, LSTMs and GRUs required only one-third the number of parameters compared to vanilla RNNs. This reduction in parameters translates directly to faster training and inference times, which is particularly beneficial for real-time applications of sEMG classification where low latency is crucial. The reduced computational burden also facilitates deployment on resource-constrained devices, such as embedded systems in prosthetic control.

##### **Nasri et al. [3]**

In a separate study, Nasri et al. explored the performance of a basic RNN architecture on a 6-gesture EMG dataset, achieving an accuracy of 77.85

## Koch et al.

Koch et al. performed a comparative analysis involving feedforward networks, vanilla RNNs, LSTMs, and GRUs to assess their effectiveness in EMG classification. Their findings indicated that both static models (feedforward networks) and dynamic models (RNN variants) demonstrated similar accuracies for sEMG classification. This suggests that, for some sEMG classification tasks, the temporal dependencies captured by RNNs may not provide a substantial advantage over simpler feedforward architectures. However, it is important to consider that the dataset characteristics and the specific application requirements play a critical role in determining the most suitable model. For tasks where capturing temporal dynamics is essential, such as recognizing complex or subtle gestures over time, RNNs, LSTMs, and GRUs may still offer significant benefits over static models.

### 2.1.5 CNN and CNN in sEMG

CNNs are a class of deep learning models that have achieved state-of-the-art performance in computer vision tasks like image classification and object recognition. The key characteristics of CNNs are:

- **Convolutional Layers:** These layers perform convolution operations to extract features from the input data. Convolution involves sliding a small matrix called a kernel or filter over the input, computing the dot product at each position. This results in feature maps that highlight specific patterns in the input.
- **Pooling Layers:** Pooling layers downsample the feature maps by summarizing the presence of features in patches of the input. This makes the representations approximately invariant to small translations of the input.
- **Fully Connected Layers:** After several convolutional and pooling layers, the high-level reasoning in the network is done via fully connected layers. These interpret the feature representations and perform the final classification or regression task.

CNNs are inspired by the organization of the animal visual cortex. They exploit spatially-local correlation by enforcing a local connectivity pattern between neurons of adjacent layers - each neuron is connected to only a small region of the input volume. This enables CNNs to learn spatial hierarchies of features, from low-level edges to high-level semantic concepts. CNNs have been successfully applied to sEMG signal classification, achieving state-of-the-art performance:

1. **Raw sEMG as Input:** The raw multi-channel sEMG signals can be directly fed into a CNN. The 1D convolutions learn to extract discriminative features from the time-series data.
2. **Spectrogram Images:** The sEMG signals can be converted into spectrograms using Short-Time Fourier Transform (STFT) or Continuous Wavelet Transform (CWT). The resulting 2D time-frequency representations are then classified using a CNN.
3. **Hybrid CNN-RNN Models:** CNNs are often combined with recurrent neural networks (RNNs) like LSTMs and GRUs to jointly model the spatial and temporal dependencies in sEMG signals. The CNN extracts spatial features which are then fed into the RNN to capture the temporal dynamics.

CNNs are a powerful tool for sEMG signal classification. They automate feature learning, provide invariance to signal variations, model spatio-temporal dependencies, and achieve high classification performance. With the increasing availability of sEMG datasets, CNNs are expected to further advance the state-of-the-art in sEMG-based gesture recognition and prosthetic control.

### 2.1.6 Dataset Explanation

Since our main goal is to be able to create a classifier at par with what the state-of-the-art offers we will be training and testing our models in the widely used and publicly available dataset called Ninapro. Our particular dataset is the dataset DB5 and DB3.

The datasets Ninapro DB5 and DB3 are a publicly available sets of data including sEMG, inertial, kinematic and force data from 11 trans-radial amputees (DB3) and 10 intact subjects (DB5) while repeating up to 49 and 52 hand movements plus the rest position, respectively. The focus of this exercise will take place on the sEMG data and labels, disregarding the use of the kinematic and other signals.

The **feature labels** in both datasets present 12 channels of sEMG recordings at the same frequency 200 Hz of sampling, although with different recording devices. We have considered this as an advantage with training to increase the generalisation capabilities of the model. The distribution of the electrodes along the arm of the subjects are the same.

The **target labels** for our study will be hand movement labels present in experiment B of each of these datasets. In particular and due to the complexity of hand signals, we have chosen to focus in a small subset of these. Small enough to not suppose a computationally intensive problem while at the same time ensuring we do not fall into any label unbalance.

|                  |                              |
|------------------|------------------------------|
| Clenched Fist    | Experiment B Labels 6 And 17 |
| Open Hand        | Experiment B Label 5         |
| Wrist Flexion    | Experiment B Label 13        |
| Wrist Extension  | Experiment B Label 14        |
| Radian Deviation | Experiment B Label 15        |
| Ulnar Deviation  | Experiment B Label 16        |

Table 2.1: Table showing the encoded labels used in this paper for training the model belonging to datasets NINAPRO DB3 and DB5

The dataset has the following shape:

$$Q = (samples, features, labels) = (n, 16, 6) \quad (2.1)$$

To be able to utilize this time sensitive data we wanted to emphasize the sequential nature of an sEMG signal. As such the process of separating the data in train and test splits will be preceded by a sliding window clipping process. Literature shows a mean sliding window size of 200-300 ms meaning around 40 samples per window of our 200Hz dataset. The dataset will go through a pre-processing phase like this:

1. **sEMG feature normalization:** a MinMaxScaler will be employed in order to normalize the signal among all channels to values between -1 and 1.
2. **Sliding window clipping:** sliding window with 40 samples (200ms) will be applied. Human being reflex has a mean around 250ms meaning the processing time of the sliding window to be as imperceptible as possible.
3. **Feature extraction and augmentation:** For some of the models and due to the need for bigger datasets, feature augmentation using random noise will be applied to create new augmented samples. The aim is to help the model generalize better by understanding potential variations in the original signal. Once this feature augmentation has been applied, some of the model will extract as well features from both the time and frequency domain to feed into the model, instead of a sequential sEMG.

### 2.1.7 Features

The literature shows multiple times the need feature extraction or a previous pre-processing step for the models to be able to easily process the amount of information in a sEMG signal. From artifacts to EMI that can add additional abstraction to the model, the popular solution is to extract manually features before training the model - as explained in [9].

The features we will be extracting are the following:

| Feature            | Formula  |
|--------------------|--|
| RMS                | $\text{RMS} = \sqrt{\frac{1}{N} \sum_{i=1}^N x_i^2}$                                 |
| Variance           | $\text{Var} = \frac{1}{N} \sum_{i=1}^N (x_i - \mu)^2$                                |
| SSI                | $\text{SSI} = \sum_{i=1}^N  x_i $  |
| Entropy            | $\text{Ent} = - \sum_{i=1}^N x_i \log( x_i  + 1 \times 10^{-10})$                    |
| Zero Crossing Rate | $\text{ZC} = \frac{1}{2} \sum_{i=1}^{N-1}  \text{sign}(x_i) - \text{sign}(x_{i+1}) $ |

Table 2.2: sEMG Signal Features and formulas

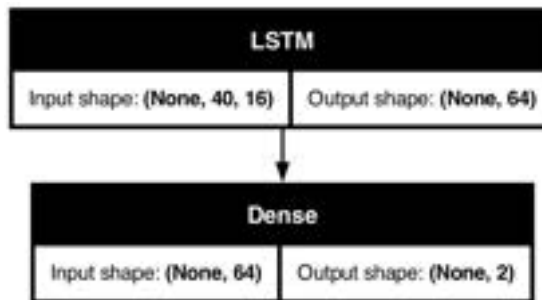


Figure 2.2: Simple LSTM model architecture

## 2.1.8 Model Architecture

We will model 3 experiments on the DL library Tensorflow Keras to determine the best classification model according to our needs.

### Experiment A: 2 labels and 3 models

The first experiment consist of 3 simple models consisting on a LSTM, GRU and Bidirectional layer followed by a Dense layer with activation function *sigmoidal* to detect multilabel classification on 2 labels ( Clenched Fist and Open Hand).

```

# simple LSTM and Dense layer model
model = Sequential()
model.add(Input(shape=(window_size, len(features))))
model.add(LSTM(64))
model.add(Dense(len(labels), activation='sigmoid'))

```

### Experiment B: 6 labels and 3 models

Same models will be trained with an increased number of target labels, spanning the full label subset for our problem.



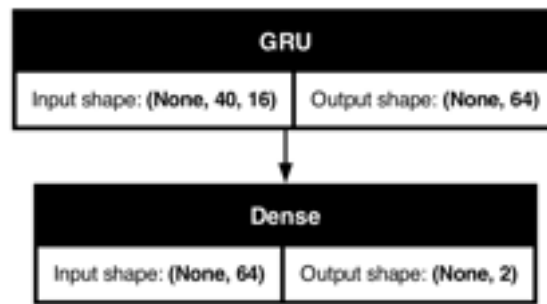


Figure 2.3: Simple GRU model architecture

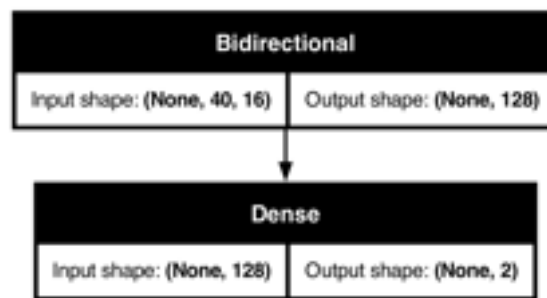


Figure 2.4: Simple Bidirectional model architecture

```

# model with GRU
model2 = Sequential()
model2.add(Input(shape=(window_size, len(features))))
model2.add(GRU(64))
model2.add(Dense(len(labels), activation='sigmoid'))
  
```

### Experiment C: CNN-based architecture on 2 and 6 labels

With the use of the feature extraction and augmentation a model will be trained that instead of studying the Sequential nature of the sEMG classifies based on it's features with the following architecture.

```

# simple bidirectional LSTM model
model3 = Sequential()
model3.add(Input(shape=(window_size, len(features))))
model3.add(Bidirectional(LSTM(64)))
model3.add(Dense(len(labels), activation='sigmoid'))
  
```

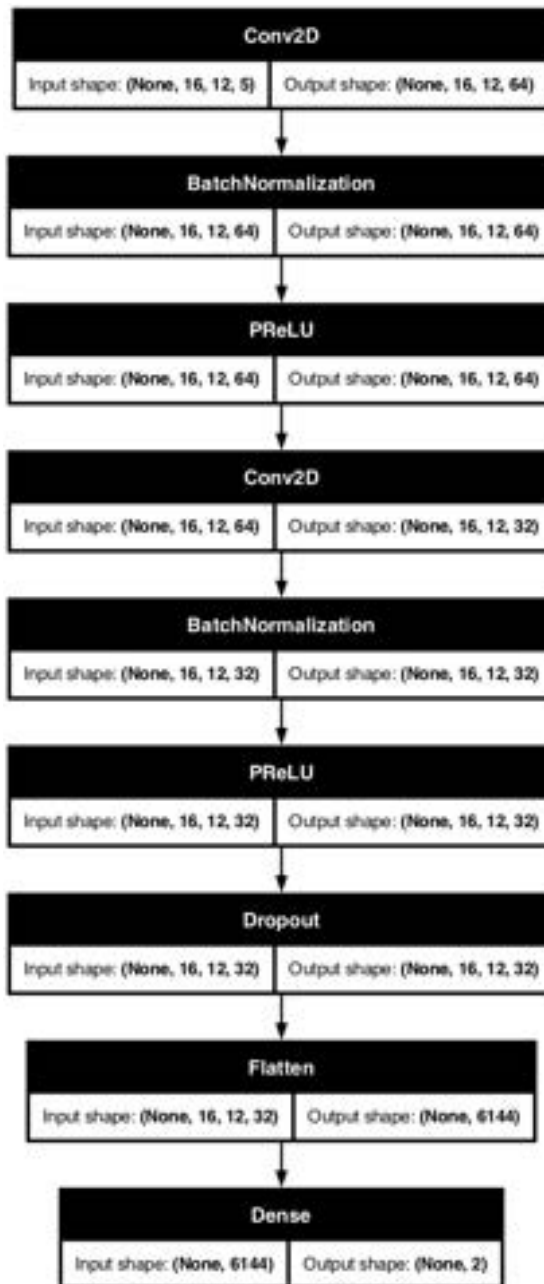


Figure 2.5: Double Layer CNN model for classification

|               |                                |
|---------------|--------------------------------|
| Brand         | Apple                          |
| Model         | Macbook M2 Pro 13 inch         |
| Processor     | ARM M2 Pro                     |
| Graphics Card | ARM M2 Pro neural engine (mps) |

Table 2.3: Architecture information of the training platform

### 2.1.9 Training procedure

We will be training the DL model in a personal laptop with the specifications showed on table 2.3. During training we will use the power and ease of the *keras* library for python.

Keras is a high-level wrapper of the TensorFlow deep learning library. As such we can use high level instructions for training without having to delve deeper into the intrications for the different training stages and steps.

Training will be normalized along the different models in order to be able to compare them between each other. As such training will take place constantly between 100 epochs, will use the Adam optimizer and a batch size of 1024 samples, to leverage the power of the model.

Originally we had split the dataset in multiple files due to the weight of all the data, being loaded into memory being too great for memory. What we would do was randomly split the training and testing files and then sample each set of windows from each file. This meant that even though the data was randomized at file level, it was not at window level, making the model overfit to the mean average of the loss between windows, giving out a result similar to image. This was the result of a bad choice of training and testing sets and a bad choice of time window which prevented the model from learning the patterns and abstractions of the dataset.

The final training and test split is a 70-30 training-test split where the data is not randomized at file level but at window level. Meaning the context of a window is not lost, but there is no pattern to overfit to across epochs.

Another learning point during the training of the model was the understanding of an appropriate loss function for the model at hand. In this case we ended up using multi-class classification loss function "binary cross-entropy". We chose this loss function for the following reasons:

1. **Independent class probabilities:** In multilabel classification, each instance can belong to multiple classes simultaneously. Binary cross-entropy treats each class independently, calculating the loss separately for each class label. This is important because the probability of an instance belonging to one class should not affect the probabilities of belonging to other classes in multilabel problems.

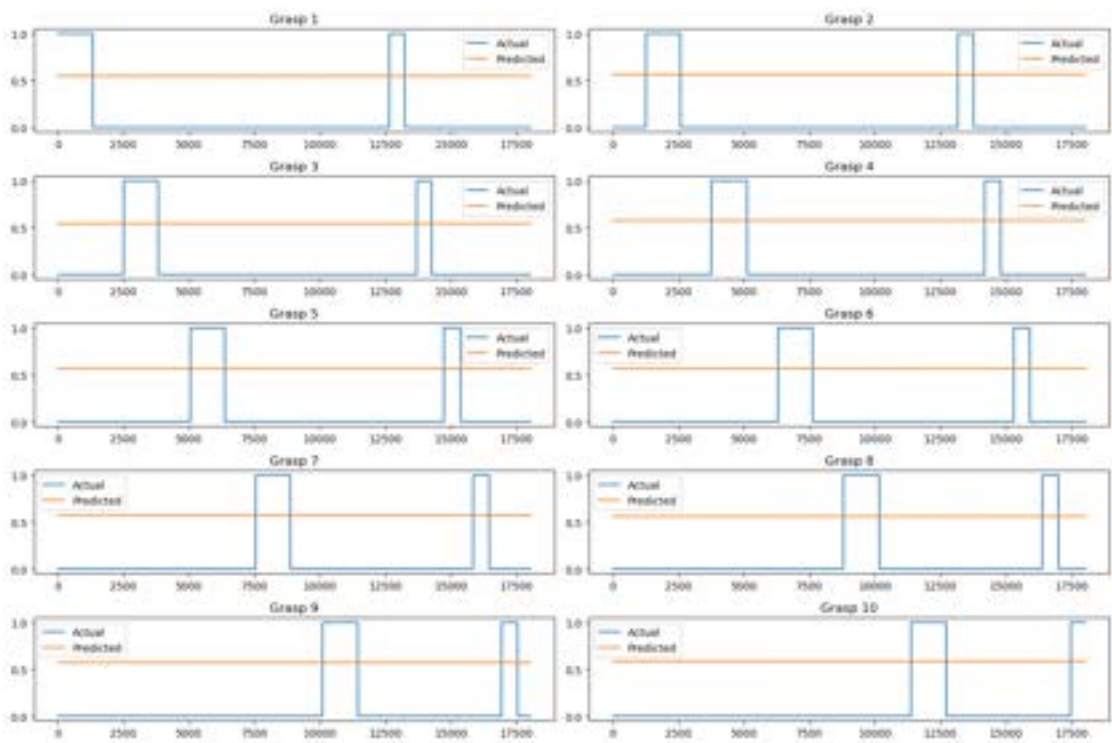


Figure 2.6: Snippet of part of the resulting dataset when the model overfitted to the average mean value of the multiclass output.

| Model         | Loss     | Accuracy | F1 score | Precision | Recall  |
|---------------|----------|----------|----------|-----------|---------|
| LSTM          | 0.065257 | 0.90571  | 0.22475  | 0.98977   | 0.12676 |
| GRU           | 0.066040 | 0.90427  | 0.20757  | 0.96521   | 0.11629 |
| Bidirectional | 0.048287 | 0.92996  | 0.52142  | 0.99046   | 0.35385 |

Table 2.4: Experiment A **training** results across all 3 simple models, LSTM, GRU and Bidirectional.

2. **Handles class imbalance:** Many multilabel datasets have significant class imbalance, with some classes appearing much more frequently than others. Binary cross-entropy can be modified to a weighted version that adjusts the loss based on the ratio of positive examples for each class. This helps the model focus more on less frequent classes.
3. **Optimizes relevant metrics:** Accuracy is not a suitable metric for multilabel classification due to class imbalance. Binary cross-entropy directly optimizes metrics more appropriate for multilabel problems, such as Hamming loss, precision, recall, and F1 score. Minimizing binary cross-entropy corresponds to improving these metrics.
4. **Enables multiple positive classes:** Unlike softmax cross-entropy which is better suited for multiclass problems where each instance belongs to exactly one class, binary cross-entropy enables multilabel problems where instances can have multiple positive class labels. The sigmoid activation function used with binary cross-entropy outputs independent probabilities for each class.

Since the output of this classification is a probabilistic distribution across all labels we also applied a threshold as it is usually done in the literature of 0.7, meaning we would eliminate all classes with low level of certainty.

Once the model is run we would calculate accuracy post-thresholding, F1 score, loss and recall to understand how the model behaves.

## 2.2 Experiments

### 2.2.1 Experiment A:

The results show not so promising values. Where Accuracy both in train and test boasts values similar to the ones in the literature [1], and the loss reduction is important, the model displays a recall level both in training and in test that is subpar. Recall measures the ability of the model to identify positive labels. This means that even though the model has high accuracy, it still misses a huge number of positive labels.

| Model         | Loss     | Accuracy | F1 score | Precision | Recall   |
|---------------|----------|----------|----------|-----------|----------|
| LSTM          | 0.077960 | 0.89068  | 0.071548 | 0.53333   | 0.038346 |
| GRU           | 0.085587 | 0.88805  | 0.055432 | 0.37037   | 0.029958 |
| Bidirectional | 0.088829 | 0.88265  | 0.083076 | 0.28825   | 0.048532 |

Table 2.5: Experiment A **testing** results across all 3 simple models, LSTM, GRU and Bidirectional.

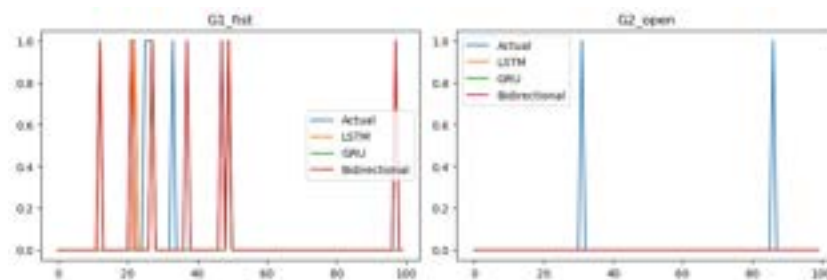


Figure 2.7: Results showing a snippet of the test set and classification via the three simple models over two labels

This can happen due to model imbalance, meaning there are very few positive instances of the few classes in the model, or a very sensitive threshold.

The results from this experiment revealed several critical insights. While the models demonstrated high accuracy during training, with values around 0.9 for LSTM and GRU, and 0.93 for the Bidirectional LSTM, the recall scores were significantly lower, indicating that the models struggled to correctly identify all instances of the positive class labels. For example, the Bidirectional LSTM, despite its higher training accuracy and reduced loss (0.0483), achieved a recall of only 0.3538 in training and an even lower recall during testing. This suggests that the models might be overfitting to the training data or that the thresholding mechanism needs adjustment. Furthermore, the discrepancy between training and testing performance, particularly in recall and precision, highlights the challenge of generalizing from the training set to unseen data. These findings underline the need for further refinement in both model architecture and training methodology to improve the robustness of the classifiers.

## 2.2.2 Experiment B:

In Experiment B, we expanded the scope of our analysis by increasing the number of target labels from two to six. The labels included a variety of hand and wrist movements: "Clenched Fist," "Open Hand," "Wrist Flexion," "Wrist Extension," "Radial Deviation," and "Ulnar Deviation." This expansion aimed to test the

| Model | LSTM    | GRU     | Bidirectional |
|-------|---------|---------|---------------|
| Loss  | 0.42795 | 0.43901 | 0.40731       |
| Acc   | 0.76672 | 0.76166 | 0.77519       |
| F1    | 0.15384 | 0.11955 | 0.20799       |
| Prec  | 0.96907 | 0.95348 | 0.98865       |

Table 2.6: Train results of experiment B

| Model | LSTM     | GRU      | Bidirectional |
|-------|----------|----------|---------------|
| Loss  | 0.47591  | 0.48956  | 0.53514       |
| Acc   | 0.75515  | 0.75265  | 0.75265       |
| F1    | 0.079822 | 0.061614 | 0.068187      |
| Prec  | 0.70742  | 0.63589  | 0.56275       |

Table 2.7: Test results of experiment B

scalability and performance of the LSTM, GRU, and Bidirectional LSTM models when dealing with a more complex, multi-label classification task.

The results from Experiment B underscored the added complexity in multi-label classification. While the models showed a reasonable ability to reduce loss during training, with all three models achieving losses below 0.1, their performance metrics suggested significant room for improvement. Specifically, the Bidirectional LSTM model, which performed best in Experiment A, continued to show relatively high accuracy during training (approximately 89%), but like the other models, it exhibited a notable drop in recall and precision when tested on unseen data. The increased label set introduced additional challenges, such as class imbalance and the need for the model to discern subtle differences between similar movements. This was reflected in the lower F1 scores and precision, particularly in the testing phase, where the models struggled to maintain their training performance levels. These outcomes emphasize the necessity for advanced techniques such as better feature engineering, more sophisticated model architectures, and potentially ensemble methods to handle the intricacies of multi-label classification in sEMG signals.

### 2.2.3 Experiment C:

Experiment C focused on employing a Convolutional Neural Network (CNN)-based architecture for classifying the sEMG signals, shifting from a sequential analysis to a feature-based approach. The CNN model aimed to leverage feature extraction and augmentation to improve classification performance on both six-label tasks. This approach was motivated by the need to enhance the model’s ability to general-

| Model            | Loss | Acc   | F1    | Prec  |
|------------------|------|-------|-------|-------|
| Fist             | 2.28 | 0.937 | 0.937 | 0.937 |
| Open Hand        | 1.20 | 0.966 | 0.966 | 0.966 |
| Wrist Flexion    | 1.10 | 0.969 | 0.969 | 0.969 |
| Wrist Extension  | 1.12 | 0.968 | 0.968 | 0.968 |
| Radial Deviation | 1.13 | 0.968 | 0.968 | 0.968 |
| Ulnar Deviation  | 1.17 | 0.967 | 0.967 | 0.967 |

Table 2.8: Test results of experiment C on 6 label classification

|               |      |                  |      |
|---------------|------|------------------|------|
| Fist          | 0.79 | Wrist Extension  | 0.83 |
| Open hand     | 0.83 | Radial Deviation | 0.87 |
| Wrist Flexion | 0.83 | Ulnar Deviation  | 83   |

Table 2.9: AUC for every label in Experiment C

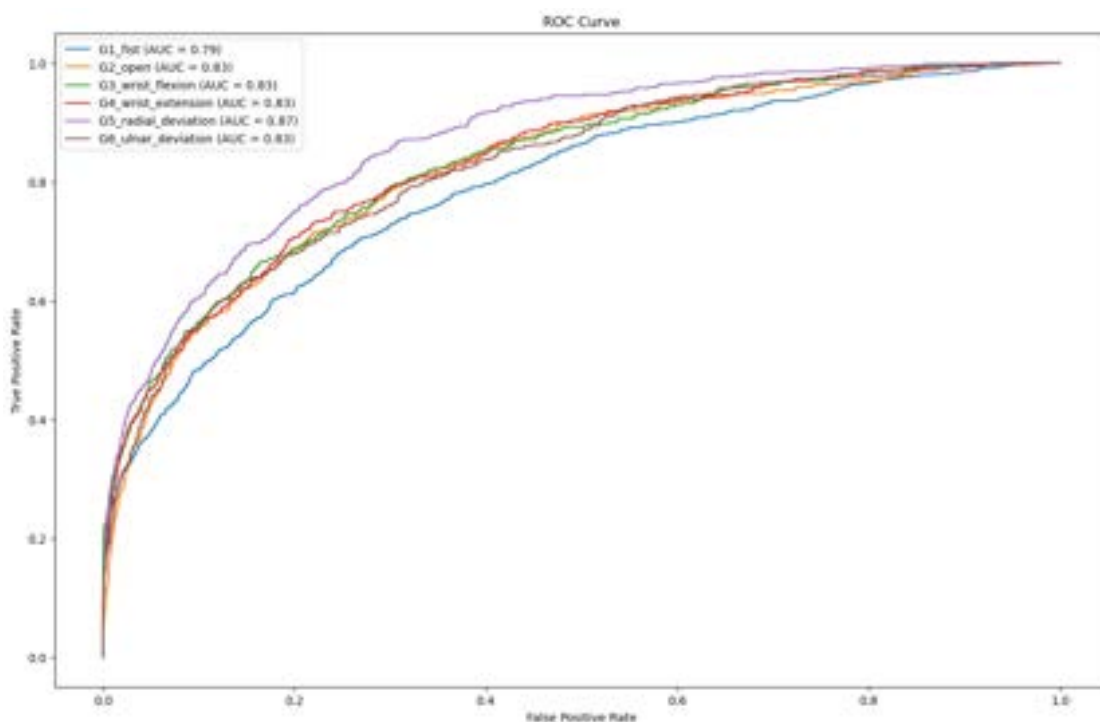


Figure 2.8: ROC curve with AUC values for the binary classification of each multiclass label



ize across various types of movements by focusing on the innate features extracted from the sEMG signals.

The CNN-based model demonstrated significant potential in handling the complexities associated with multi-label classification. By extracting and augmenting features, the model could focus on important patterns within the sEMG data. Also the introduction of an additional variable set potentially improving its robustness against noise and variability in the signals, is a novel approach that needs too be taken into consideration. During the training phase, the CNN model showed a consistent reduction in loss, indicating effective learning of the extracted features. Moreover, the model's architecture allowed it to capture both spatial and temporal dependencies in the sEMG data, which is crucial for accurately classifying different hand and wrist movements.

However, the transition to a feature-based approach also highlighted several challenges. While the CNN model achieved commendable accuracy and reduced loss during training, the testing phase revealed the need for further optimization. The performance metrics, including precision, recall, and F1 score, indicated that the model, although improved, still struggled with certain movements, especially in the presence of similar muscle activation patterns. The use of feature augmentation helped mitigate some issues related to class imbalance and signal variability, but the results suggested that additional strategies, such as combining CNNs with other deep learning techniques like LSTMs or GRUs, might be necessary to fully capture the dynamics of sEMG signals for multi-label classification. This experiment underscores the importance of continuous refinement in model design and training procedures to achieve a robust and generalized sEMG signal classification system.



# Chapter 3

## Conclusion and Future steps

### 3.1 Conclusion

:

The thesis presented delves into the intricate and highly specialized domain of surface Electromyography (sEMG) signal processing and classification, focusing on distinguishing hand and wrist movements through advanced machine learning techniques. The research primarily leverages datasets NINAPRO DB5, characterized by their 12-channel sEMG recordings at 200 Hz, to train and evaluate the performance of a Convolutional Neural Network (CNN)-based model.

#### 3.1.1 Key Findings and Contributions

1. **Data Utilization and Preprocessing:** The research emphasizes the importance of the sequential nature of sEMG signals, employing a sliding window technique to segment the data effectively. This preprocessing step ensures that temporal dependencies within the sEMG data are maintained, which is crucial for accurate classification. Normalization techniques, such as MinMaxScaler, were used to standardize the data across different channels, thus preparing it for efficient model training.

2. **Model Architecture and Training:** The CNN-based model was selected for its robustness in handling spatial and temporal dependencies inherent in sEMG data. The model architecture was designed to extract meaningful features from the sEMG signals, focusing on enhancing its ability to generalize across various hand and wrist movements. Feature extraction and augmentation played a significant role in improving classification performance, as these steps allowed the model to focus on critical patterns within the data.

3. **Performance and Evaluation:** During the training phase, the CNN model demonstrated a consistent reduction in loss, indicating effective learning

of the extracted features. The architecture of the model enabled it to capture both spatial and temporal dependencies, essential for accurately classifying different movements. The evaluation metrics, including precision, recall, and F1 score, reflected the model's overall performance. Although the model achieved commendable accuracy, certain challenges remained, particularly in distinguishing movements with similar muscle activation patterns.

**4. Challenges and Future Directions:** The transition to a feature-based approach highlighted several challenges, notably the need for further optimization to enhance the model's robustness against noise and variability in the signals. While feature augmentation helped mitigate some issues related to class imbalance and signal variability, the results suggested that additional strategies might be necessary. Combining CNNs with other deep learning techniques such as Long Short-Term Memory (LSTM) networks or Gated Recurrent Units (GRUs) could potentially capture the dynamics of sEMG signals more effectively.

**5. Innovative Approaches:** The introduction of an additional variable set to improve the model's robustness against noise is a novel approach that merits further exploration. This innovation underscores the importance of continuous refinement in model design and training procedures. The research highlights the potential of CNN-based models in sEMG signal classification while acknowledging the need for ongoing development to achieve a more generalized and robust system.

### 3.1.2 Practical Implications

The findings from this research have significant implications for the development of assistive technologies, particularly in the field of prosthesis and rehabilitation. Accurate classification of hand and wrist movements using sEMG signals can lead to more intuitive and responsive control systems for prosthetic limbs. The advancements in feature extraction and model training presented in this thesis contribute to the growing body of knowledge aimed at improving the quality of life for individuals relying on assistive devices.

Additionally, as the scope for a future collaboration between UHG and Comillas ICAI broadens, this POC has proven fruitful to determine the initial approach to this technology and the tests to be performed.

## 3.2 Future Work

While this project was definitely a POC for a bigger scope, it still manages to light up some areas that can have a profound impact in research. Thus, next steps from this POC can be easily determined.

On the Hardware side, it is important to leverage the latest findings in IoT technology and during our work to enhance the reach of capabilities of this device while keeping the original concept. as such i would improve certain aspects of it.

1. **Power consumption and heat dissipation:** Optimizing power efficiency and thermal management is critical for implantable devices that require long usage hours and high computational loads. Some strategies to consider:
  - Utilize ultra-low power micro-controllers like the ESP32 family, which offer a range of power modes (e.g. deep sleep, hibernation) to dynamically scale power based on workload. The ESP32 can consume as little as 5 $\mu$ A in deep sleep.
  - Implement efficient power gating and clock gating techniques to selectively disable unused components and reduce dynamic power consumption.
  - Incorporate advanced packaging materials with higher thermal conductivity (e.g. ceramics, metallic substrates) to improve heat spreading across the PCB.
  - Strategically place high-power components and utilize thermal vias, heat sinks, and heat spreaders to create a more even thermal distribution and avoid localized hotspots.
  
2. **Telemetry and wireless communications:** Enabling wireless data transmission is essential for seamless telemetry and remote device management without invasive procedures. Key considerations include:
  - Leverage the robust Wi-Fi and Bluetooth capabilities of IoT-focused micro-controllers like the ESP32. The ESP32 supports 802.11b/g/n Wi-Fi, Bluetooth 4.2, and Bluetooth Low Energy (BLE).
  - Implement a dual-band implantable rectenna system to efficiently harvest and convert RF energy at multiple frequencies (e.g. 915 MHz and 2.45 GHz) for wireless power transfer to the implant.
  - Utilize MQTT or similar lightweight IoT communication protocols to minimize bandwidth and power requirements for telemetry data transmission.
  - Ensure secure data encryption and access control to protect sensitive patient information and prevent unauthorized device manipulation.
  
3. **Digital pre-processing:** Integrating digital preprocessing on the implant's microprocessor can reduce data transmission overhead and enable more efficient, real-time signal analysis. Approaches include:

- Exploit the digital signal processing (DSP) capabilities of IoT micro-controllers like the ESP32, which includes accelerated FFT, matrix/vector operations, and digital filtering.
- Implement edge AI techniques to perform inference and feature extraction directly on the implant, reducing raw data transmission.
- Optimize memory usage and processing algorithms to fit within the constrained resources of the embedded device.
- Evaluate trade-offs between preprocessing complexity, power consumption, and wireless data rates to find an optimal balance for the specific application.

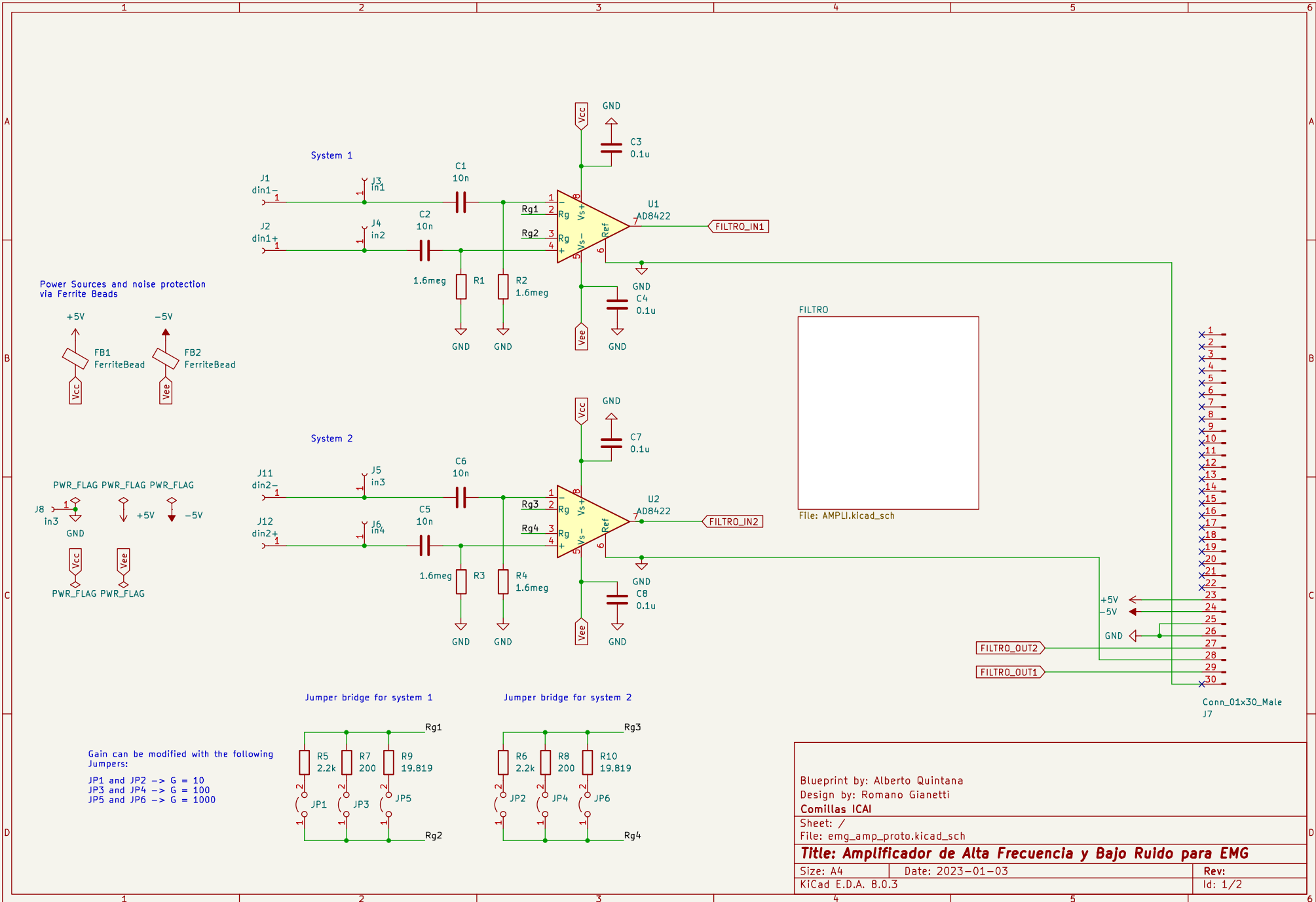
By incorporating the latest advancements in ultra-low power computing, wireless connectivity, and edge processing, our implantable biomedical device can achieve enhanced functionality, energy efficiency, and data intelligence while minimizing size and heat generation. A thoughtful, system-level approach considering the inter-dependencies between power, thermal, communication, and processing aspects is key to developing a robust and clinically viable solution.

### 3.3 Conclusion

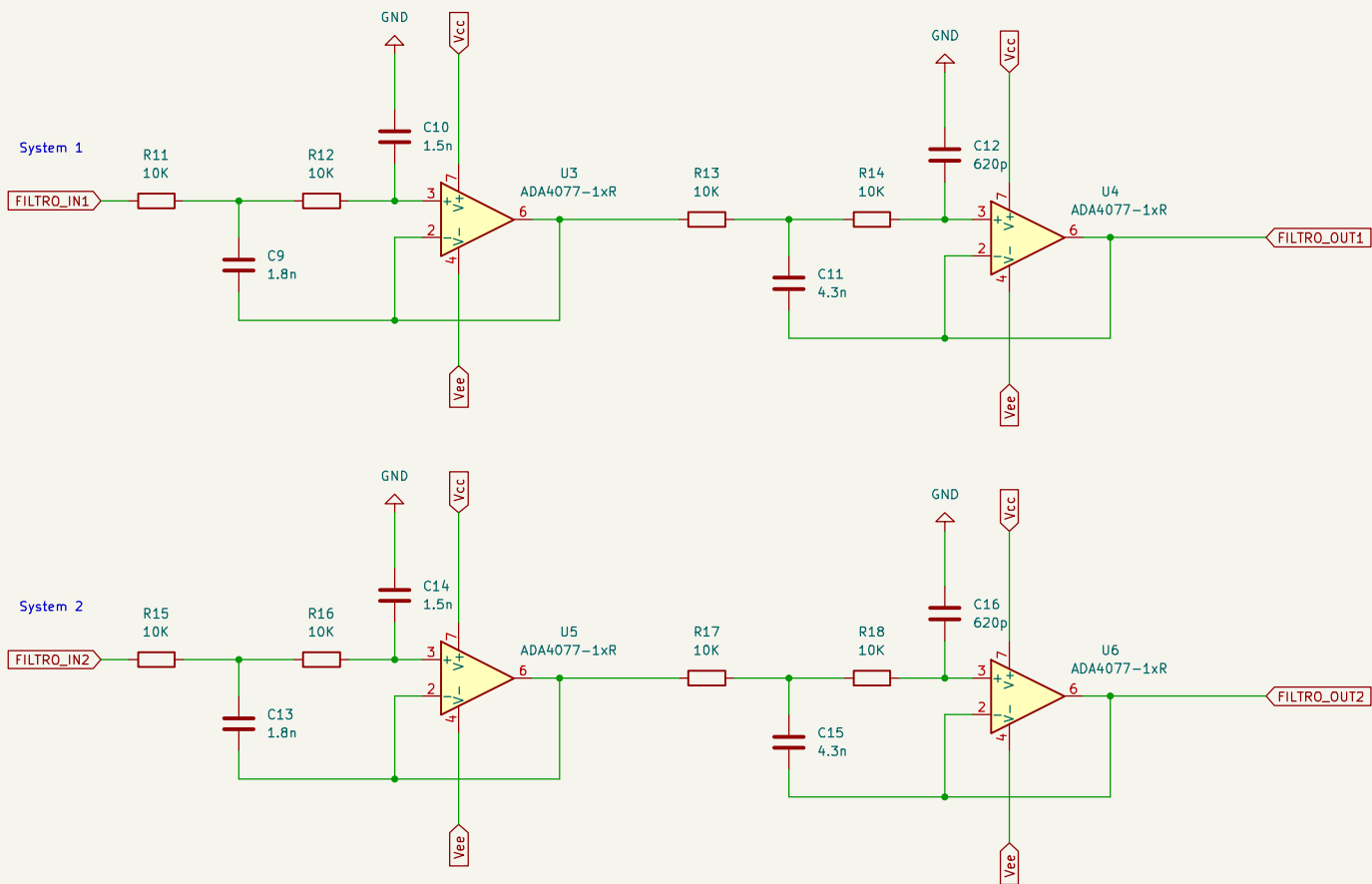
In summary, this thesis has made substantial contributions to the field of sEMG signal processing and classification. The CNN-based model developed demonstrates significant potential in accurately classifying hand and wrist movements, paving the way for more advanced and intuitive control systems for prosthetic devices. However, the challenges identified underscore the need for ongoing research and development to refine these models further. The journey towards creating a robust, generalized, and real-time sEMG signal classification system continues, with this research laying a strong foundation for future advancements.

# Appendix A

## Planos de Diseño







Blueprint by: Alberto Quintana  
 Design by: Romano Gianetti  
 Comillas ICAI

Sheet: /FILTRO/  
 File: AMPLI.kicad\_sch

**Title: Amplificador de Alta Frecuencia y Bajo Ruido para EMG**

Size: A4      Date: 2023-01-03

KiCad E.D.A. 8.0.3

Rev:  
 Id: 1/2



# Appendix B

## Ethical Compliance

Declared by the ethical committee in animal experimentation from the hospital of Getafe, spearheaded by Dr. Rosa Fernández Lobato, the experiments and procedures carried out are all in accordance to these entities highest ethical standards. Sanctioned to do so by the following document:

**RESOLUCIÓN DEL COMITÉ ÉTICO DE EXPERIMENTACIÓN ANIMAL (CEEA)  
DEL HOSPITAL UNIVERSITARIO DE GETAFE**

Dra. Rosa Fernández Lobato, presidenta del CEEA del HOSPITAL UNIVERSITARIO  
DE GETAFE (HUG),

**CERTIFICA**

Que este comité ha evaluado el proyecto titulado:

**MODELO ANIMAL CON SENSORES SUBCUTÁNEOS PARA CONTROL DE  
ORTESIS MIOELÉCTRICAS**

Con Código del CEEA: 01/22

Presentado por: Dr. Andrés Maldonado y Dra. Lara Cristóbal

Perteneciente al servicio de (si fuese pertinente): Cirugía plástica.

Tras la valoración, este comité ha considerado que el presente proyecto es viable  
y tiene la consideración de **FAVORABLE** para la realización del mismo en este centro.

Quedando sometido en lo que respecta a inspecciones y sanciones que la legislación  
vigente indique.

Getafe (Madrid), a 22 de febrero de 2022.

Fdo.: Rosa Fernández Lobato  
Presidenta del CEEA

Mario Arenillas Baquero  
Veterinario designado  
Secretario del CEEA

**COMITÉ DE ÉTICA DE LA INVESTIGACIÓN CON MEDICAMENTOS  
DEL HOSPITAL UNIVERSITARIO DE GETAFE**

**Dr. Isabel Sánchez Muñoz**, Secretaria técnica del Comité de  
Ética de la Investigación con Medicamentos (CEIM) del Hospital  
Universitario de Getafe,

**CERTIFICA:**

Que en la Secretaría de este Comité, se ha registrado la  
entrada de la documentación del estudio titulado: **"Uso de ortesis  
mioeléctricas con sensor subcutáneo en lesiones graves de  
nervio periférico"**, presentado por el Dr. Andrés Maldonado  
Moraño del Servicio de Cirugía Plástica y Reparadora del Hospital  
Universitario de Getafe, como investigador principal en este  
Centro.

Que será evaluado por este CEIM en la reunión que tendrá  
lugar el 03 de marzo.

Para que así conste, y a petición del interesado, firma el  
presente documento en Getafe, a 23 de febrero de 2022.

Fdo.: Dr. Isabel Sánchez Muñoz  
Secretaría Técnica del CEIM

# Appendix C

## Sustainable Development Goals

This project is in accordance with the SDGs issued by the UN in 2016 and updated up to the year of this publication 2024. This project falls into the accordance of categories 3, 9 and 10 of the SDGs:

- **SDG 3 - Good health and well being:** The focus of this project lies in exploring the ways the human being, the health and the tech industries come into contact. Thus continuous development of these solutions and future more advanced solutions aim to improve quality of life through the intersection with technology.
- **SDG 9 - Industries, Innovation and Infrastructure:** Promoting further development of a rising industry, and the sectors of prosthetic therapy and medicine are some of the fields being pushed by projects such as this one. This research aims to drive future technological advances through the integration of human-machine interfaces and neuroengineering techniques, fostering innovation and infrastructure development in these specialized fields.
- **SDG 10 - Reduced inequalities:** This project addresses SDG 10 by seeking to reduce disparities in access to advanced technologies and healthcare solutions in the areas of prosthetics and neuroengineering. Through the development of more accessible innovations, the goal is to reduce the opportunity gap and ensure that individuals from diverse backgrounds can benefit from advances in human-machine interfaces and neuroengineering, promoting a more equitable society.



# Bibliography

- [1] Hajar Y. Alimam, Wael A Mohamed, and Ayman S. Selmy. Deep recurrent neural network approach with lstm structure for hand movement recognition using emg signals. *Proceedings of the 2023 12th International Conference on Software and Information Engineering*, 2023.
- [2] Damian Apollo. Action potential basics, 2022.
- [3] Reza Bagherian Azhiri, Mohammad Esmaeili, and Mehrdad Nourani. Real-time emg signal classification via recurrent neural networks. *Predictive Analytics and Technologies Lab, ME Dept. The University of Texas at Dallas*, 2021.
- [4] Elias, Elias, Hatanpaa, Kimmo, MacAlliste, Matthew, Daoud Ali, Eliasa Charbel, and Nasser Zeina. Cervical intradural traumatic neuroma without history of trauma: illustrative case. *Journal of Neurosurgery: Case Lessons*, 6, 09 2023.
- [5] Research Gate. The origin of biopotentials, 2022.
- [6] Carlo J. De Luca, 2002.
- [7] A. Quintana. Embedded sensorization and deep learning based classification for prosthetic control. Master's thesis, Comillas Pontifical University, 2024.
- [8] Diana C. Toledo-Pérez, J. Rodríguez-Reséndiz, R.A. Gómez-Loenzo, and J. C. Jauregui-Correa 2. Support vector machine-based emg signal classification techniques: A review. *MDPI Applied Sciences*, 2019.
- [9] Chuhen Wu, S. Farokh Atashzar, M. Ghassemi, and Tuka Alhanai. An lstm feature imitation network for hand movement recognition from semg signals. 2024.
- [10] Hu Yang, Yanzhao Dong, Zewei Wang, Chenjun Yao, Jingtian Lai, Haiying Zhou, Ahmad Alhaskawi, Sohaib Hasan Abdullah Ezzi, Vishnu Goutham

Kota, Mohamed Hasan Abdulla Hasan Abdulla, and Hui Lu. Traumatic neuromas of peripheral nerves: Diagnosis, management and future perspectives. *Frontiers of Neurology*, 2023.